MOLECULAR AND CELLULAR BIOLOGY, Dec. 2006, p. 9517–9532 Vol. 26, No. 24
0270-7306/06/$08.00+0 doi:10.1128/MCB.01145-06

Perk-Dependent Translational Regulation Promotes Tumor Cell Adaptation and Angiogenesis in Response to Hypoxic Stress▽†

Jaime D. Blais,[1,2] Christina L. Addison,[1] Robert Edge,[1,2] Theresa Falls,[1] Huijun Zhao,[1] Kishore Wary,[4] Costas Koumenis,[5] Heather P. Harding,[6] David Ron,[6] Martin Holcik,[3] and John C. Bell[1]*

Ottawa Health Research Institute, 501 Smyth Rd., Ottawa, Ontario K1H 8L6, Canada[1]; Department of Biochemistry, University of Ottawa, Ottawa, Ontario, Canada[2]; Apoptosis Research Centre, Children's Hospital of Eastern Ontario, 401 Smyth Rd., Ottawa, Ontario K1H 8L1, Canada[3]; Department of Pharmacology, University of Illinois at Chicago, 835 S. Wolcott, Room E403, Chicago, Illinois 60612[4]; Department of Radiation Oncology, University of Pennsylvania School of Medicine, 185 John Morgan Building, 3620 Hamilton Walk, Philadelphia, Pennsylvania 19104-6072[5]; and Skirball Institute, New York University School of Medicine, New York, New York 10016[6]

Received 26 June 2006/Returned for modification 10 August 2006/Accepted 20 September 2006

It has been well established that the tumor microenvironment can promote tumor cell adaptation and survival. However, the mechanisms that influence malignant progression have not been clearly elucidated. We have previously demonstrated that cells cultured under hypoxic/anoxic conditions and transformed cells in hypoxic areas of tumors activate a translational control program known as the integrated stress response (ISR). Here, we show that tumors derived from K-Ras-transformed Perk$^{-/-}$ mouse embryonic fibroblasts (MEFs) are smaller and exhibit less angiogenesis than tumors with an intact ISR. Furthermore, Perk promotes a tumor microenvironment that favors the formation of functional microvessels. These observations were corroborated by a microarray analysis of polysome-bound RNA in aerobic and hypoxic Perk$^{+/+}$ and Perk$^{-/-}$ MEFs. This analysis revealed that a subset of proangiogenic transcripts is preferentially translated in a Perk-dependent manner; these transcripts include VCIP, an adhesion molecule that promotes cellular adhesion, integrin binding, and capillary morphogenesis. Taken with the concomitant Perk-dependent translational induction of additional proangiogenic genes identified by our microarray analysis, this study suggests that Perk plays a role in tumor cell adaptation to hypoxic stress by regulating the translation of angiogenic factors necessary for the development of functional microvessels and further supports the contention that the Perk pathway could be an attractive target for novel antitumor modalities.

The presence of hypoxic cells in solid tumors is well documented, and clinical and experimental evidence suggests that the hypoxic microenvironment of a tumor promotes a more aggressive phenotype by selecting for the clonal expansion of apoptotically insensitive cells (28). Growing tumors are often exposed to heterogeneous environments with regions of solid tumors containing microenvironmental niches deficient of critical metabolites, such as oxygen and glucose (11). Indeed, low oxygenation can accelerate malignant progression and metastasis, resulting in a poorer prognosis irrespective of the chosen treatment regimen (38). The ability of tumor cells to survive and adapt to hypoxic microenvionments can be attributed to the regulation of several key mechanisms, including the loss of pathways that can induce cell death (28), the stimulation of angiogenesis to increase tumor oxygenation (87), and the capability to strictly regulate energy homeostasis (37). Energy conservation is crucial to cellular survival, as ATP production is diminished by the lack of oxidative phosphorylation. Thus, hypoxic stress results in a rapid metabolic shift that favors anaerobic glycolysis and the inhibition of high-energy-consuming processes, including protein translation (75).

The control of mRNA translation is emerging as an important cellular response to stress that can assert a significant influence on individual gene expression (9, 22, 31, 48, 50, 65, 79). Hypoxia results in a rapid and reversible inhibition in global protein synthesis to help alleviate energy demands when oxygen and ATP levels are low; however, the exact mechanisms controlling translational regulation are not fully understood. While early responses to hypoxia involve the activation of Perk and transient phosphorylation of the alpha subunit of translation initiation factor 2 (eIF2α) (7, 9, 51), translational inhibition appears to occur in distinct phases and to involve multiple pathways (16, 50, 59). Exposure to hypoxia activates the endoplasmic reticulum (ER)-resident kinase Perk, resulting in the phosphorylation of eIF2α and the adaptive modulation of protein synthesis and gene expression through a signal transduction pathway referred to as the integrated stress response (ISR) (35), an arm of the unfolded protein response (UPR) that facilitates the cellular adaptation to ER stress. Translational repression is mediated by phosphorylation of serine 51 of eIF2α, resulting in decreased ternary complex formation and, subsequently, decreased translation initiation. An important function of the UPR is to reduce the demand on the protein-folding machinery within the ER to protect the cell from ER stress. Inhibiting translation not only conserves ATP but also helps to decrease the client load in the ER. Translational inhibition paradoxically leads to the selective translation

* Corresponding author. Mailing address: Ottawa Health Research Institute, 503 Smyth Rd., 3rd floor ORCC, Ottawa, ON K1H 1C4, Canada. Phone: (613) 737-7700, ext. 70439. Fax: (613) 247-3524. E-mail: jbell@ohri.ca.

† Supplemental material for this article may be found at http://mcb.asm.org/.

▽ Published ahead of print on 9 October 2006.

of several mRNAs necessary for the survival and adaptation of cells to cellular stress, including the transcription factor ATF4 (9, 31). ATF4 transcriptionally activates stress-responsive genes which encode proteins that are necessary to resolve the UPR, including Gadd34, BiP, and CHOP (31, 61). The physiological significance of Perk signaling is underscored by the observation that $Perk^{-/-}$ mice are viable at birth but die quickly due to early onset diabetes caused by the rapid destruction of secretory cells resulting from accumulated unfolded proteins (32). Furthermore, cells with compromised Perk and eIF2α signaling are significantly more sensitive to ER-induced cell death than wild-type cells (32, 33, 84, 102). The critical role for Perk in tumor cell adaptation to hypoxic stress is underscored by our observation that, in its absence, cells are incapable of initiating the integrated stress response during oxygen deprivation, thus leading to a loss in tumor cell viability (7). Moreover, $Perk^{-/-}$ tumors are substantially smaller than $Perk^{+/+}$ tumors, and they exhibit decreased survival in response to hypoxic stress (7). In this study, we demonstrate that tumors derived from K-Ras-transformed $Perk^{-/-}$ mouse embryonic fibroblasts (MEFs) are not only smaller than wild-type tumors but also appear to have severe limitations in their ability to stimulate angiogenesis. Using a mouse model of angiogenesis, we assessed the significance of Perk within the tumor microenvironment on vessel formation and maturation. We demonstrate that $Perk^{+/+}$ tumors facilitated endothelial cell survival and functional vessel formation, whereas $Perk^{-/-}$ tumors formed more nonfunctional, irregularly structured vessels that led to hemorrhaging within the tumor matrix. These findings are supported by a microarray analysis of polysome-bound mRNAs, which demonstrated that Perk affects the translation of numerous angiogenic genes during hypoxic stress. Included in the cohort of genes identified was an adhesion protein, *v*ascular endothelial growth factor (VEGF) and type 1 *c*ollagen *i*nducible *p*rotein (VCIP), that promotes cell adhesion, spreading, and integrin binding within the tumor endothelium (41, 42). These findings help to establish that Perk is a key posttranscriptional regulator that is capable of inducing the expression of a collection of genes necessary for the cellular adaptation to hypoxic stress. This work further supports the notion that the ISR represents an attractive target for novel antitumor therapies that may help overcome the development of hypoxia tolerance in tumors.

MATERIALS AND METHODS

Cell culture and generation of stable cell lines. Simian virus 40 (SV40)-immortalized and K-Ras-transformed $Perk^{+/+}$ and $Perk^{-/-}$ MEFs were maintained in Dulbecco modified Eagle medium supplemented with 10% fetal calf serum, 55 μM β-mercaptoethanol, and 10 μM nonessential amino acids. Human dermal microvascular endothelial cells (HDMECs) were cultured in microvascular endothelial cell growth medium (EGM-2MV; Cambrex). The generation of stable clones overexpressing the alkaline phosphatase (AP) protein was as previously described (71).

Proliferation assay. Five thousand K-Ras-transformed $Perk^{+/+}$ or $Perk^{-/-}$ MEFs were plated in a 24-well dish. Cells were counted by hemocytometer every 24 h for 5 days. Results are representative of three independent experiments counted in triplicate.

Constructs. The bicistronic vectors, beta-galactosidase (β-Gal)/encephalomyocarditis virus (EMCV)/chloramphenicol acetyltransferase (CAT) (containing the internal ribosome entry site [IRES] for EMCV), β-Gal/EMPTY/CAT (empty vector control), and HP–β-Gal/EMPTY/CAT (hairpin-containing empty vector), were described previously (39, 96). The human VCIP 5′ untranslated region (5′UTR) was cloned into the XhoI site of the intercistronic region between the β-Gal and CAT cistrons in both β-Gal/EMPTY/CAT and HP–β-Gal/EMPTY/CAT. The VCIP 5′UTR deletion constructs were assembled by using a QuikChange II XL site-directed mutagenesis kit (Stratagene) per the manufacturer's instructions.

Hypoxia treatments. All experiments were performed with exponentially growing cells. For all experiments with the exception of polysome fractionation, cells were plated in 60-mm glass culture dishes at a density of $\sim 1 \times 10^6$ cells/plate. After approximately 20 h, the culture dishes were placed in a hypoxic culture chamber (MACS VA500 microaerophilic workstation; Don Whitley Scientific, Shipley, United Kingdom). Hypoxic conditions were achieved with 90% N_2, 5% CO_2, and 5% H_2 (anaerobic grade gas) and palladium catalysts to scavenge trace oxygen.

Isolation of polysomes and RNA. Polysome fractionation and RNA isolation were performed as previously described (9).

Microarray analysis. Microarray analysis was performed as previously described (9). Briefly, RNA from the high-molecular-weight polysomes (fractions 6 to 10) was pooled from the normoxic samples (hereafter called 0 h poly) and from hypoxic samples (hereafter called 4 h poly). Prior to microarray analysis, RNA from the polysome fractions and the total RNA from the cytoplasmic lysates (0 h total and 4 h total) were purified using an RNeasy kit (QIAGEN, Mississauga, Canada), per the manufacturer's instructions. Twenty micrograms of each RNA sample was processed according to the manufacturer's standard protocol (Affymetrix, Santa Clara, Calif.) and hybridized to an Affymetrix mouse 430_2 gene chip. Data were analyzed using Genespring software (Silicon Genetics, Redwood City, Calif.).

Total cellular changes and polysome analysis. The analysis of total cellular mRNA and polysome-associated mRNAs was performed as described previously (9). To identify genes that are preferentially translated in a Perk-dependent manner during hypoxic stress, we compared the mean signal intensities of the $Perk^{+/+}$ 0 h poly gene chip to the 4 h poly gene chip and the $Perk^{-/-}$ 0 h poly gene chip to the 4 h poly gene chip using a mean cutoff of 1.5-fold. Genes that demonstrated a concomitant increase in total mRNA expression (>2-fold change in the 4 h total gene chip relative to the 0 h total gene chip) were removed. Using Genespring software (Silicon Genetics), we created Venn diagrams to make a list of hypoxia-responsive translationally regulated candidates that were induced exclusively in the $Perk^{+/+}$ cells relative to the $Perk^{-/-}$ cells. Genes were further categorized based on known or proposed molecular functions and sorted by the ratio of 4 h poly signal/0 h poly signal, which was used as a basis for interpreting the efficiency of translation during hypoxic stress.

Quantitative RT-PCR. The aforementioned total and polysomal RNA from hypoxic (4 h) and normoxic treated $Perk^{+/+}$ and $Perk^{-/-}$ cells was reverse transcribed (1 μg RNA) in the presence of 40 ng of vesicular stomatitis virus RNA encoding the M protein (VSV-M) RNA (a viral transcript used as a control for reverse transcription [RT] efficiency and quantitative PCR [Q-PCR]). Q-PCR was performed in triplicate to amplify all targets by using a FastStart DNA Master SYBR Green I kit (Roche Diagnostics, Laval Canada) per the manufacturer's instructions and a Roche LightCycler thermocycler. Crossing points were converted to absolute quantities based on standard curves generated for each target amplicon. All target signals were subsequently normalized to VSV-M in order to correct for RT-PCR efficiency.

Primers. The primers used were as follows: mGADD34 (forward, CTGCAAGGGGCTGATAAGAG; reverse, AGGGGTCAGCCTTGTTTTCT), mATF3 (forward, CAGAGCCTGGTGTTGTGCTA; reverse, GGTGTCGTCCATCCTCTGTT), mVCIP (forward, CCTCTTCTGCCTCTTCATGG; reverse, GCCACATACGGGTTCTGAGT), mGrb10 (forward, CTGGCTGACCTGGAAGAAAG; reverse, TCAGAAACACTGCGCATAGG), mHyou1 (forward, ACCTAGAGAAGCGGGAGAGG; reverse, GCTTGTCCTTCAGCATCACA), mIGFBP2 (forward, ACAACGAGCAGCAGGAGACT; reverse, CAGAAGCAAGGGAGGTTCAG), mMMP13 (forward, ATCCTGGCCACCTTCTTCTT; reverse, TTTCTCGGAGCCTGTCAACT), and mCol6a (forward, CCTGCTCAGCCAGTCCTTAC; reverse, GACTTCTCGGGACACTCTCG).

Q-PCR results are presented as the number of transcripts per μg of total RNA or polysomal RNA. Results from each transcript were normalized to an exogenous control mRNA (VSV-M).

β-Galactosidase and CAT analysis. Cells were washed in phosphate-buffered saline (PBS) and harvested in CAT enzyme-linked immunosorbent assay kit lysis buffer (Roche Molecular Biochemicals) per the manufacturer's instructions. β-Galactosidase enzymatic activity in cell extracts was determined as previously described (63). CAT levels were determined using a CAT enzyme-linked immunosorbent assay kit (Roche Molecular Biochemicals) per the manufacturer's instructions. The relative IRES activity was determined as the ratio of CAT/β-Gal in a minimum of three independent experiments.

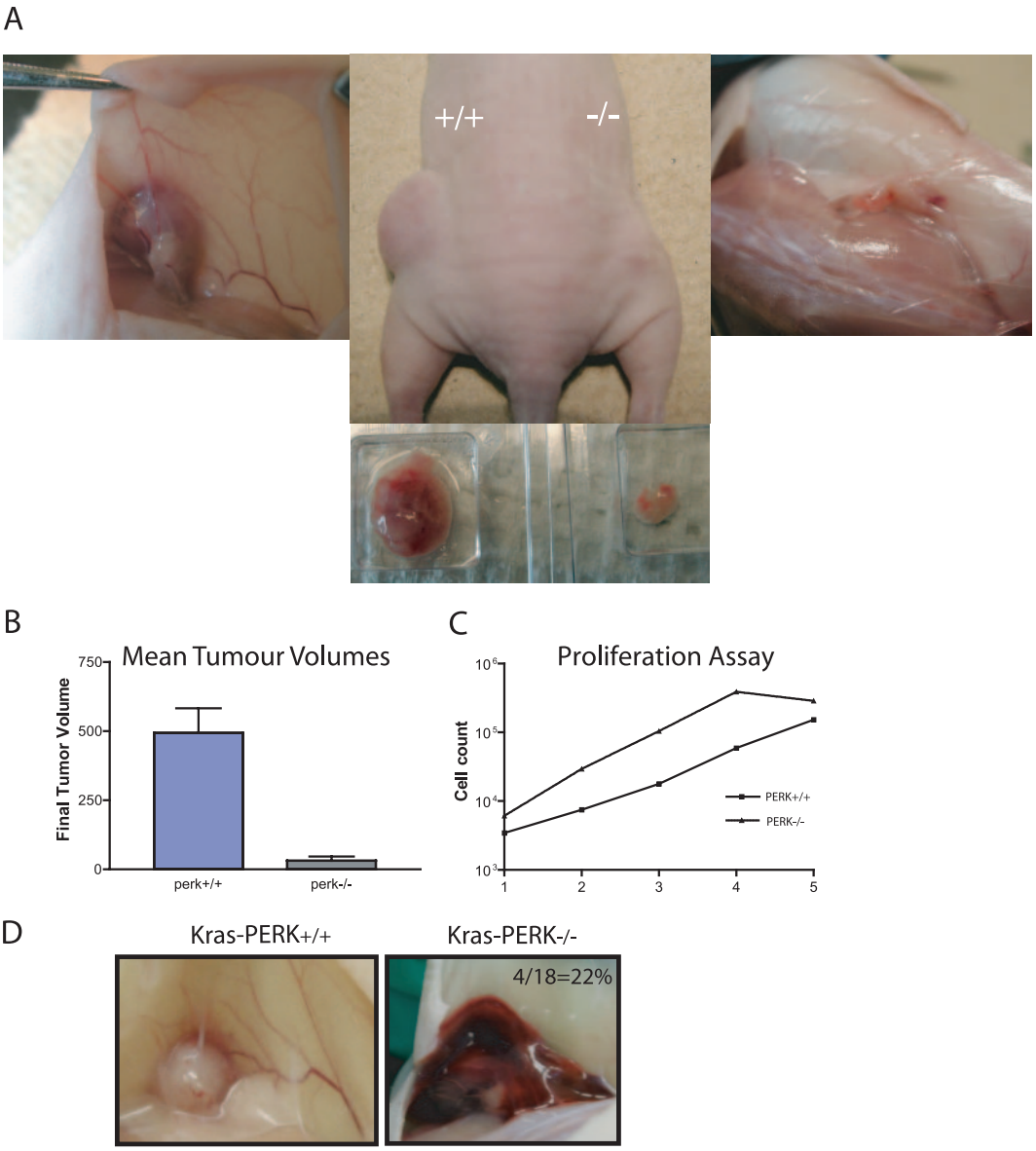

FIG. 1. Perk affects tumor growth and angiogenesis in vivo. (A) Middle frame, representative nude mouse injected with Perk$^{+/+}$ K-Ras MEFs (left flank) and Perk$^{-/-}$ K-Ras MEFs (right flank) with 5×10^5 cells/site, at sacrifice. The dissected tumors are displayed below. Left and right frames, photographs of Perk$^{+/+}$ (left) and Perk$^{-/-}$ (right) tumors during dissection. Note the number of vessels migrating towards the Perk$^{+/+}$ tumor compared to the Perk$^{-/-}$ tumor. (B) Final tumor volumes (cm^3) from seven animals at sacrifice, 23 to 41 days following subcutaneous inoculation of tumor cells (means ± standard errors of the means [SEM]). (C) Growth rates of K-Ras-transformed Perk$^{+/+}$ and Perk$^{-/-}$ MEFs in vitro ($n = 3$). (D) Two representative photographs from nude mice at sacrifice following a subcutaneous injection of 5×10^5 K-Ras-transformed Perk$^{+/+}$ (left) or Perk$^{-/-}$ MEFs (right). Note the hemorrhagic pocket surrounding the Perk$^{-/-}$ tumors. Upon dissection, tumors within these blood-filled pockets remained small, pale nodules.

Measurement of spurious splicing and cryptic promoter activity. Total RNA was isolated from U2OS cells transfected with the β-Gal/EMCV/CAT, β-Gal/EMPTY/CAT, or β-Gal/VCIP/CAT reporter plasmid and reverse transcribed using SuperScript II (Invitrogen). Quantitative PCR was performed in triplicate to amplify all targets by using a FastStart DNA Master SYBR Green I kit (Roche Diagnostics, Laval Canada) per the manufacturer's instructions and a Roche LightCycler thermocycler.

Primers used were β-Gal (5′-ACTATCCCGACCGCCTTACT-3′, 5′-CTGTAG CGGCTGATGTTGAA-3′) and CAT (5′-GCGTGTTACGGTGAAAACCT-3′, 5′-GGGCGAAGAAGTTGTCCATA-3′), as described previously (38a).

Xenograft tumor model. Athymic Nu/Nu mice (Charles River Labs) were subcutaneously injected with 5×10^5 transformed Perk$^{+/+}$ and Perk$^{-/-}$ MEFs or HT.29Puro and HT.29PerkΔC cells in 100 μl of PBS. Tumors were monitored daily. Final tumor volumes were determined following tumor resection based on the formula V = length × width × depth.

Biodegradable polymer matrix. Porous polylactic acid sponges were a gift of D. Mooney (Harvard) and were prepared as previously described (67). The day prior to implantation, the sponges were soaked in 100% ethanol for 2 h followed by two washes in PBS. The sponges were soaked overnight in PBS prior to the embedding of cells.

Tumor/endothelial cell sponge implants. Prior to sponge transplantation, 9×10^5 HDMECs overexpressing AP (AP-HDMECs) and 1×10^5 Perk$^{+/+}$ or Perk$^{-/-}$ K-Ras-transformed MEFs were resuspended in 18 μl of a 1:1 mixture of growth factor-reduced Matrigel (Collaborative Biomedical Products, Cambridge, Massachusetts) and allowed to adsorb into the prepared sponges. The sponges were incubated for 30 min at 37°C to allow for the gelation of Matrigel. Nude

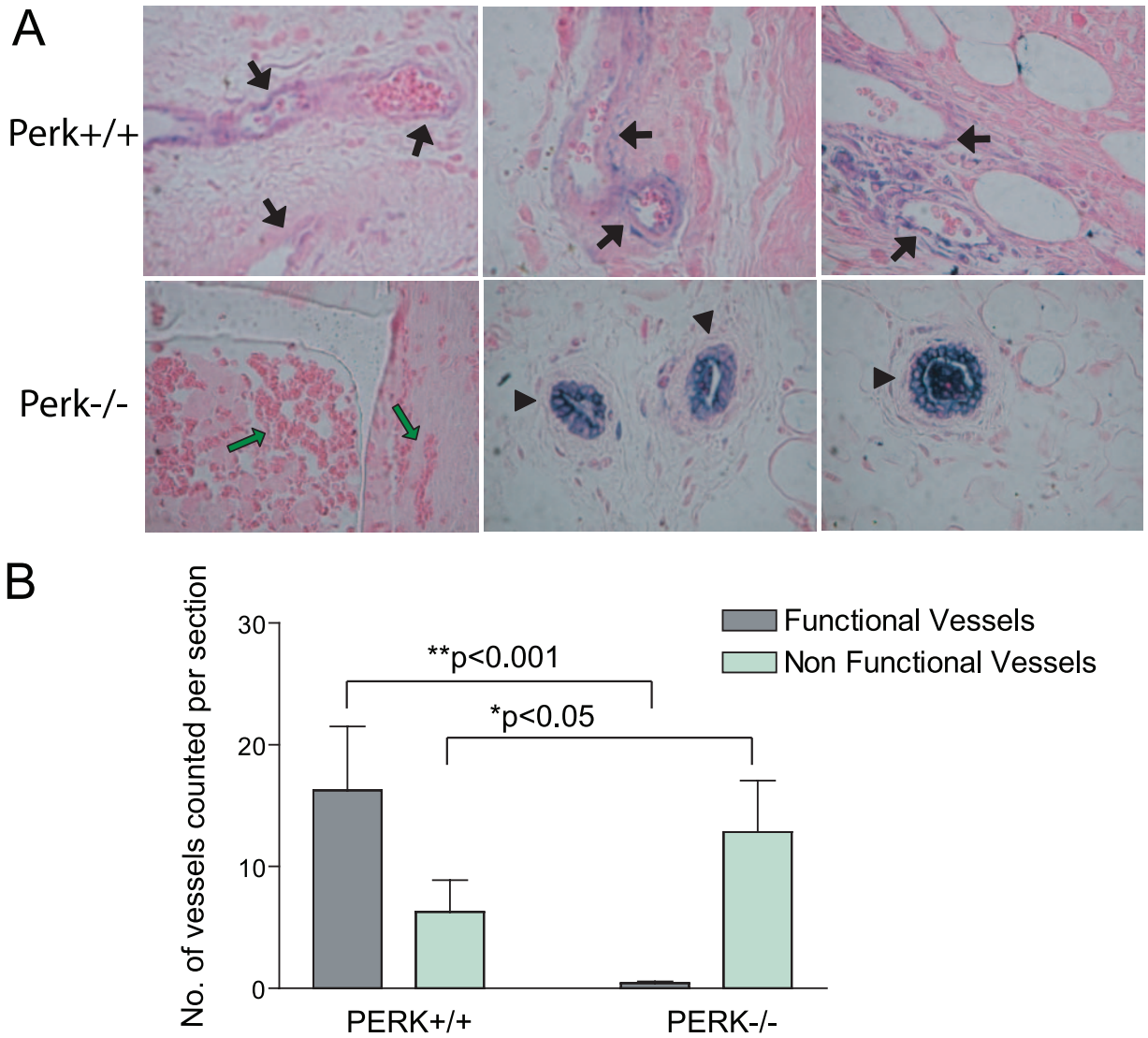

FIG. 2. Perk affects microvessel formation in vivo. (A) Paraffin-embedded AP-stained sponges were sectioned (4 μm), eosin counterstained, and visualized by light microscopy. Top panels, representative pictures from Perk$^{+/+}$ and AP-HDMEC-inoculated Matrigel/sponge implants. Bottom panels, representative pictures from Perk$^{-/-}$ and AP-HDMEC-inoculated Matrigel/sponge implants. Black arrows indicate AP-expressing functional vessels so designated by the presence of red blood cells within the vessel. Black arrowheads demonstrate nonfunctional vessels so designated by the cuboidal shape of the AP-expressing endothelial cells. Green arrows indicate hemorrhagic red blood cell infiltration. All pictures were taken at ×40 magnification. (B) The number of functional and nonfunctional vessels per section was quantified by visualization under ×40 magnification with a light microscope. The bars represent the means ± SEM from three Perk$^{+/+}$- and four Perk$^{-/-}$-containing sponges measured from three serial sections.

mice were anesthetized with isofluorane, and one sponge was implanted subcutaneously in the dorsal region of each mouse. Twenty-one days after transplantation, the mice were sacrificed and the implants were retrieved. The implants were fixed overnight in 10% buffered formalin at room temperature. Sponges were cut in half, and one half was stained for alkaline phosphatase. Unstained sections were paraffin embedded for subsequent histological evaluation.

Staining for alkaline phosphatase. Following fixation, sponges were washed three times in PBS at room temperature and once in PBS at 65°C for 30 min to inactivate any endogenous phosphatase activity. This was followed by a wash in AP buffer (100 nM Tris HCl [pH 8.5], 100 mM NaCl, 50 nM $MgCl_2$) for 10 min at room temperature. The sponge slices were stained in a solution of BCIP (5-bromo-4-chloro-3-indolyl-phosphate)/nitroblue tetrazolium chloride (Sigma) overnight at room temperature in the dark. The reaction was stopped with 20 mM EDTA in PBS, and the slices were embedded in paraffin for histological evaluation. Four-micron sections were obtained, counterstained with eosin, and visualized using an Olympus BX50 light microscope. Pictures were captured with a Nikon Coolpix 100 digital camera.

Statistics. Unless otherwise noted, data are reported as means ± standard deviations. Statistical significance was determined using Student's *t* test where appropriate, and *P* values of less than 0.05 were considered significant.

RESULTS

Perk contributes to tumor growth and angiogenesis in vivo. Inactivation of ISR signaling by mutations in the ER kinase Perk (dn-PerkΔC, Perk$^{-/-}$ MEFs) and the translation initiation factor eIF2α (eIF2α^{S51A}) impairs cell survival and results in diminished tumor growth in vivo, suggesting that the pres-

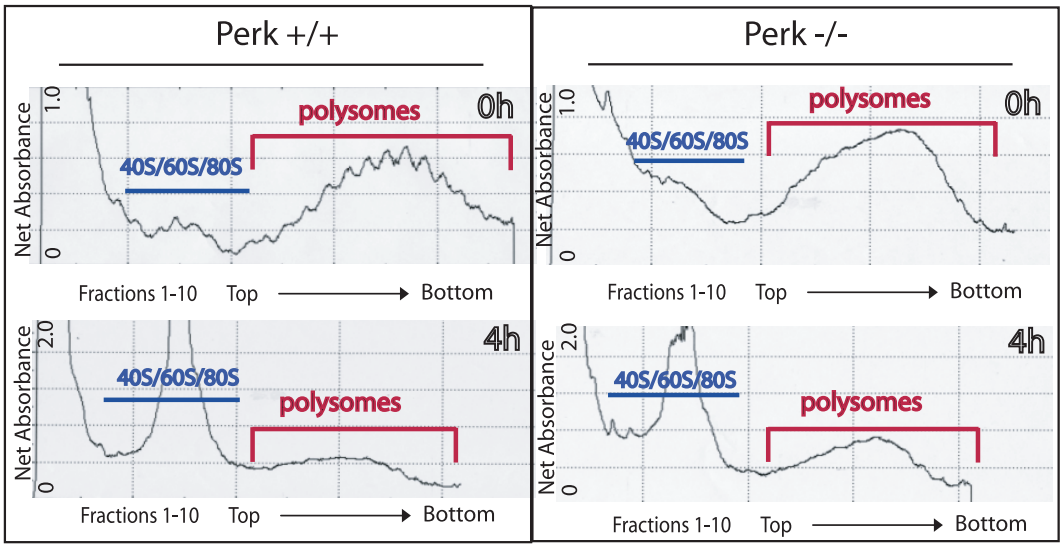

FIG. 3. Translational inhibition in response to hypoxic stress is reduced in Perk$^{-/-}$ MEFs. Polysome profiles (absorbance at 254 nm) in cell lysates fractionated by sucrose density ultracentrifugation. SV40-immortalized Perk$^{+/+}$ and Perk$^{-/-}$ cells were exposed to hypoxic stress for 4 h or left untreated (0 h). Cells were treated with cycloheximide (100 μg/ml) (37°C, 3 min) and lysed in a Triton X-100 buffer (4°C). Cell lysates were layered on a 10-ml continuous sucrose gradient (10 to 50%) and ultracentrifuged in an SW-41 rotor 39K for 90 min. The positions of the polysomes and ribosomal subunits are indicated. The increase in monosome-bound transcripts and ribosomal subunits, combined with the decrease in polysomes apparent in the hypoxia-treated cells, is indicative of decreased protein translation.

ence of Perk can increase the ability of transformed MEFs to survive and adapt to the tumor microenvironment (7). To examine the contribution of Perk to these processes, we used in vivo model systems as follows: Perk$^{+/+}$ and Perk$^{-/-}$ K-Ras-transformed MEFs were injected subcutaneously in the hind limb of nude mice. Measurements of tumor volumes were determined after tumor resection and demonstrate that Perk$^{+/+}$ tumors were, on average, 16 times larger than Perk$^{-/-}$ tumors (Perk$^{+/+}$, 493.4 ± 88.7 cm^3; Perk$^{-/-}$, 30.8 ± 15.8 cm^3; $P < 0.001$) (Fig. 1B). Interestingly, we observed upon tumor dissection that Perk$^{-/-}$ tumors appeared to have severe limitations in their ability to stimulate angiogenesis (Fig. 1A). While Perk$^{+/+}$ tumors developed rapidly and became highly vascularized, tumors that lacked Perk remained as small, pale, poorly vascularized nodules (Fig. 1A, top left panel versus top right panel). A number of Perk$^{-/-}$ tumors demonstrated severe hemorrhaging in a confined area containing the tumor (Fig. 1D). However, upon resection, these tumors were also small and appeared poorly vascularized. Similar observations were made previously for nude mice implanted with HT29 cells expressing a dominant negative mutant allele of Perk (C. Koumenis, unpublished observations). Whether the growth of Perk$^{-/-}$ tumors is limited solely by an increase in their apoptotic index, as previously suggested, or if a compromised ability to induce adaptive pathways, including angiogenesis, has a measurable effect on tumor growth had not yet been elucidated prior to this study. In vitro growth kinetic studies demonstrated that K-Ras-transformed Perk$^{-/-}$ MEFs displayed growth kinetics similar to those of Perk$^{+/+}$ MEFs, if not more advantageous (Fig. 1C); therefore, differences in tumor growth are not due to differences in in vitro proliferation rates. We would thus hypothesize that the differential responses of Perk$^{+/+}$ and Perk$^{-/-}$ cells to the tumor microenvironment influences their survival, growth, and adaptive potential.

Perk affects endothelial cell survival and vessel formation in vivo. In order to study how Perk expression modulates angiogenesis and affects tumor growth, we used a mouse model of angiogenesis in which polylactic acid sponges seeded with K-Ras-transformed Perk$^{+/+}$ or Perk$^{-/-}$ cells along with AP-HDMECs were subcutaneously implanted in nude mice. Perk expression resulted in a higher intratumoral vascular density of AP-expressing human microvessels (Fig. 2A and B). Interestingly, the microenvironment provided by the Perk$^{-/-}$ tumors resulted in significantly fewer functional AP-expressing human microvessels (Fig. 2B). Although AP-HDMEC cells formed tubule structures, the endothelial cells remained cuboidal in shape, and the centers of many of these tubules remained filled with other AP-HDMEC cells (Fig. 2A), suggesting that the consequence of disrupting Perk signaling within the tumor microenvironment results in disrupted angiogenic signals that prevent the appropriate organization and maturation of HDMECs into functional vessels (Fig. 2B). This account is further supported by the repeated observation that masses of red blood cells, in the absence of any discernible vessels, can be seen permeating the tumor matrix, perhaps due to leaky and incomplete vascular assembly (Fig. 2A, green arrows) along with the observation that Perk$^{-/-}$ tumors are frequently highly hemorrhagic (Fig. 1D). These studies suggest that the tumor microenvironment provided in a Perk-expressing tumor can promote endothelial cell survival and vascular maturation, resulting in functional vessel formation, tumor growth and, ultimately, the development of hypoxia tolerance.

Microarray analysis of polysome-bound mRNAs reveals a role for Perk in the translational regulation of angiogenic genes during hypoxic stress. We performed a microarray analysis of polysome-associated Perk$^{+/+}$ and Perk$^{-/-}$ SV40-immortalized MEFs in order to identify a cohort of genes that are translationally regulated by Perk, which may play an essential

TABLE 1. PERK-dependent translationally regulated genes

Function	Fold change for induction in:				Gene name and description	Reference(s)
	$Perk^{+/+}$ cells		$Perk^{-/-}$ cells			
	Translational	Transcriptional	Translational	Transcriptional		
Regulation of cell growth	3.9	1.9	None	None	Igfbp2: insulin-like growth factor binding protein 2	83
	3.2	1.5	1.5	1.2	Nov: nephroblastoma overexpressed gene	
Blood vessel formation	4.1	2.0	1.0	2.0	VCIP: VEGF and type I collagen inducible protein	42
Cell adhesion	2.9	0.9	0.8	1.1	D7Ertd458e: poliovirus receptor	
	2.4	0.7	None	None	Thbs2: thrombospondin 2	10, 19
	3.6	1.4	None	None	cspg2: chondroitin sulfate proteoglycan 2 (versican)	13
	2.0	0.8	0.8	0.9	col6a3: procollagen, type VI, alpha 3	86
	2.4	0.8	None	None	col12a1: collagen, type XII, alpha 1	
	0.9	0.3	2.0	2.0	EEMP1: EGF-containing fibulin-like extracellular matrix protein 1	49
Collagen catabolism	2.1	0.4	None	None	mmp13: matrix metalloproteinase 13	1
	1.1	1.1	3.2	2.8	TIMP3: tissue inhibitor of metalloproteinase 3	78
Regulation of transcription	2.2	0.9	1.0	1.5	Aebp1: AE binding protein 1	
Ephrin receptor activity	None	None	2.6	0.7	EphA4: ephrin receptor A4	99
Protein trasportation/folding	2.5	1.5	None	None	ptprm: protein tyrosine phosphatase receptor type M	
	2.2	1.4	1.1	1.9	Rrbp1: ribosome binding protein 1	
	2.1	1.1	0.9	1.5	hyou1: hypoxia up-regulated 1 (ORP150)	73
	2.8	1.0	0.9	1.0	slitl2: slit-like 2	
	2.1	0.7	1.4	2.0	plod1: procollagen-lysine 1 2-oxoglutarate 5-dioxygenase 1	
	2.1	1.2	1.4	1.0	lamp2: lysosomal membrane glycoprotein 2	
Transporter activity	2.0	0.3	0.7	0.8	aqp1: aquaporin 1	
Signal transduction	2.1	1.5	1.3	0.7	Grb10: growth factor receptor-bound protein 10	68
	2.5	1.0	1.0	3.7	pdgfrb: platelet-derived growth factor receptor beta	
	2.4	0.8	None	None	stmn2: stathmin-like 2	
Unknown	4.6	None	None	None	dcn: decorin	
	2.5	1.0	0.5	2.1	zfp503: zinc finger protein 503	
	2.1	0.9	0.7	0.8	tnc: tenascin C	
	2.1	1.5	0.6	0.8	crlf1: cytokine receptor-like factor 1	

Results of microarray analyses to identify transcripts that were associated exclusively with high-molecular-weight polysomes in SV40-immortalized $Perk^{+/+}$ MEFs following an acute response to hypoxic stress (4 h). Genespring 5.0 software was used to compare the relative expression of polysome-bound mRNAs from $Perk^{+/+}$ and $Perk^{-/-}$ MEFs following acute normoxia (0 h poly) or hypoxia (4 h poly)-treated cells. Genes were exclusively induced >1.5-fold in the polysomes of $Perk^{+/+}$ MEFs (4 h poly/0 h poly signal) and showed either a decrease or no significant change in their polysome association in $Perk^{-/-}$ MEFs (4 h poly/0 h poly signal). Candidates that demonstrated less than a twofold change in total cellular mRNA (4 h total/0 h total signal) were considered for further analysis. These genes were functionally clustered, and subsets of them are represented in this table. References are given for candidates with a described role in angiogenesis.

role in the adaptive response to hypoxic stress. We isolated mRNAs from the high-molecular-weight polysomes (fractions 6 to 10) and total cellular mRNAs from SV40-immortalized $Perk^{+/+}$ and $Perk^{-/-}$ MEFS exposed to normoxia or severe hypoxia (4 h, <0.01%) (for brevity, hypoxia in the text denotes severe hypoxia). The optical density polysome profiles are shown in Fig. 3 and demonstrate a significant inhibition in protein synthesis following hypoxic stress, as evidenced by a reduction in polysome-associated mRNAs and by the accumulation of free mRNA and rRNA, with a considerable increase in the monosome peak. Although $Perk^{-/-}$ cells demonstrate an inhibition in translation during hypoxic stress, this response is notably stronger in $Perk^{+/+}$ cells, which demonstrate a more significant decrease in polysome-associated messages (Fig. 3; compare $Perk^{+/+}$ 4 h polysomes to $Perk^{-/-}$ 4 h polysomes). That this observation has been reported by several groups (7,

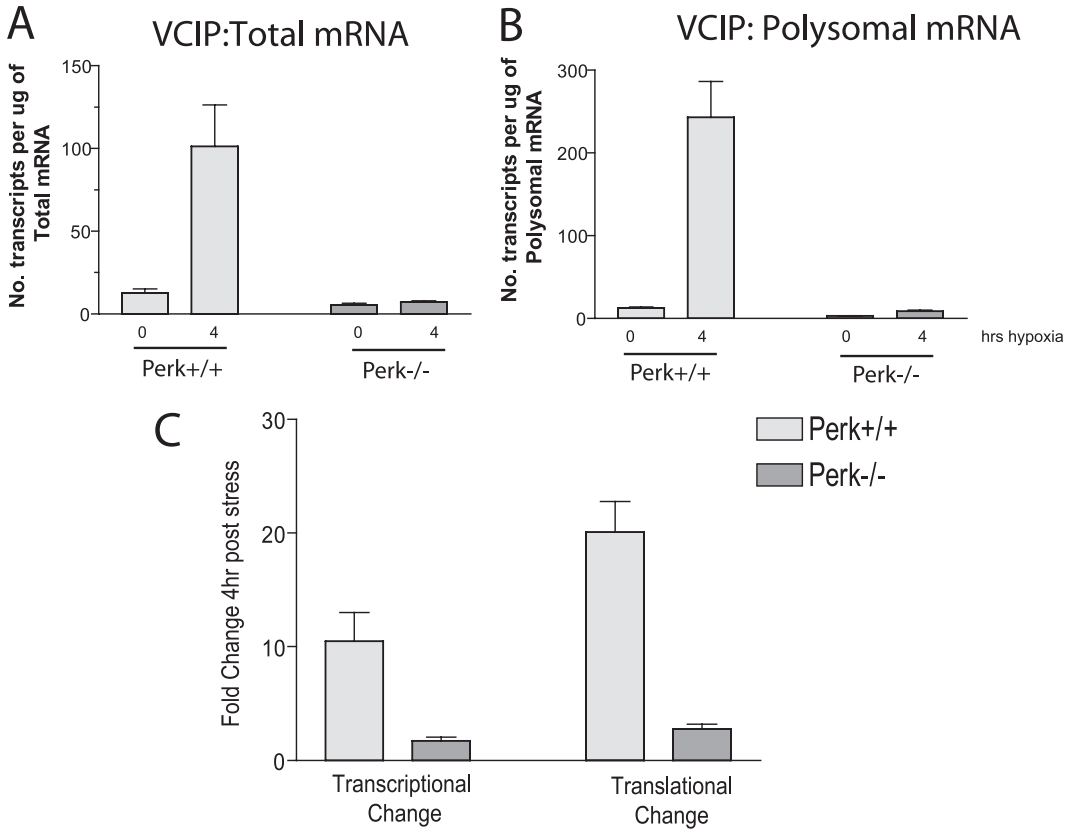

FIG. 4. VCIP mRNA is more efficiently translated during hypoxia in Perk$^{+/+}$ cells. (A) Total mRNA expression is unaffected by hypoxia. Total RNA was isolated prior to sucrose gradient fractionation from hypoxia-treated (4 h) or normoxic (0 h) SV40-immortalized Perk$^{+/+}$ and Perk$^{-/-}$ cells, reverse transcribed, and quantified by real-time PCR. The quantities of each transcript are described as the number of transcripts isolated per microgram of total RNA. Each sample was independently normalized to a spiked internal control. Q-PCR analysis was replicated in triplicate. Results are representative of the averages ± SEM for three independent experiments. (B) VCIP transcripts are enriched in the polysomes of Perk$^{+/+}$ cells during hypoxia. High-molecular-weight polysomes from hypoxia-treated (4 h) or normoxic (0 h) SV40-immortalized Perk$^{+/+}$ and Perk$^{-/-}$ cells were pooled (fractions 6 to 10), reverse transcribed, and quantified by real-time PCR. The quantities of each transcript are described as the number of transcripts isolated per microgram of polysomal RNA. Each sample was independently normalized to a spiked internal control. Q-PCR analysis was repeated in triplicate. Results are representative of the averages ± SEM for three independent experiments. (C) Perk$^{+/+}$ cells demonstrate induced translation of VCIP during hypoxia. The transcriptional change (*n*-fold) was plotted as the number of VCIP transcripts isolated per microgram of total RNA from hypoxia-treated (4 h) versus normoxic (0 h) cytoplasmic lysates. The translational change (*n*-fold) was plotted as the number of VCIP transcripts isolated per microgram of polysomal RNA from hypoxia-treated (4 h) versus normoxic (0 h) lysates.

59) substantiates an essential role for Perk in the regulation of translation initiation during acute hypoxic stress. We used microarray analysis to compare the gene expression profiles from total cellular mRNAs and polysome-associated mRNAs from the Perk$^{+/+}$ and Perk$^{-/-}$ SV40-transformed MEFs. We tailored our analysis to identify genes that displayed a hypoxia- and Perk-dependent increase in their translational efficiency as determined by their induced presence in the polysomes without a large change in total cellular mRNA levels. Successful candidates displayed an induced polysome association in Perk$^{+/+}$ cells without a concomitant induction in the total cytoplasmic mRNA pool, while polysome-associated gene expression in Perk$^{-/-}$ cells remained unchanged or decreased in response to hypoxic stress (see Fig. S2 in the supplemental material). Additionally, we sought genes that were translationally repressed by hypoxic stress in Perk$^{+/+}$ cells and demonstrated translational induction in Perk$^{-/-}$ cells. Genes that met these requirements were functionally clustered and are displayed in Table 1.

Data from our microarray substantiated the observations made with the Perk$^{-/-}$ tumors, as our analysis identified the Perk-dependent differential regulation of a cohort of proangiogenic genes. Therefore, the disruption of Perk within the tumor microenvironment may result in aberrant angiogenic signals from multiple pathways, thereby contributing to the development of poorly vascularized tumors. Notably, many of the genes identified by this analysis have been implicated in multiple pathways involved in tumor angiogenesis, including cell-cell adhesion, matrix remodeling, and extracellular matrix proteolysis.

VCIP and other angiogenic factors are efficiently translated during hypoxic stress in Perk$^{+/+}$ cells. We used Q-PCR to verify the translational regulation of six candidate genes identified by our microarray analysis (Fig. 4 and 5; see Fig. S1 in the supplemental material). Q-PCR values were normalized to an internal control, VSV-M, added exogenously to each RT reaction. With the exception of VCIP, translationally regulated array candidates demonstrated a redistribution into the poly-

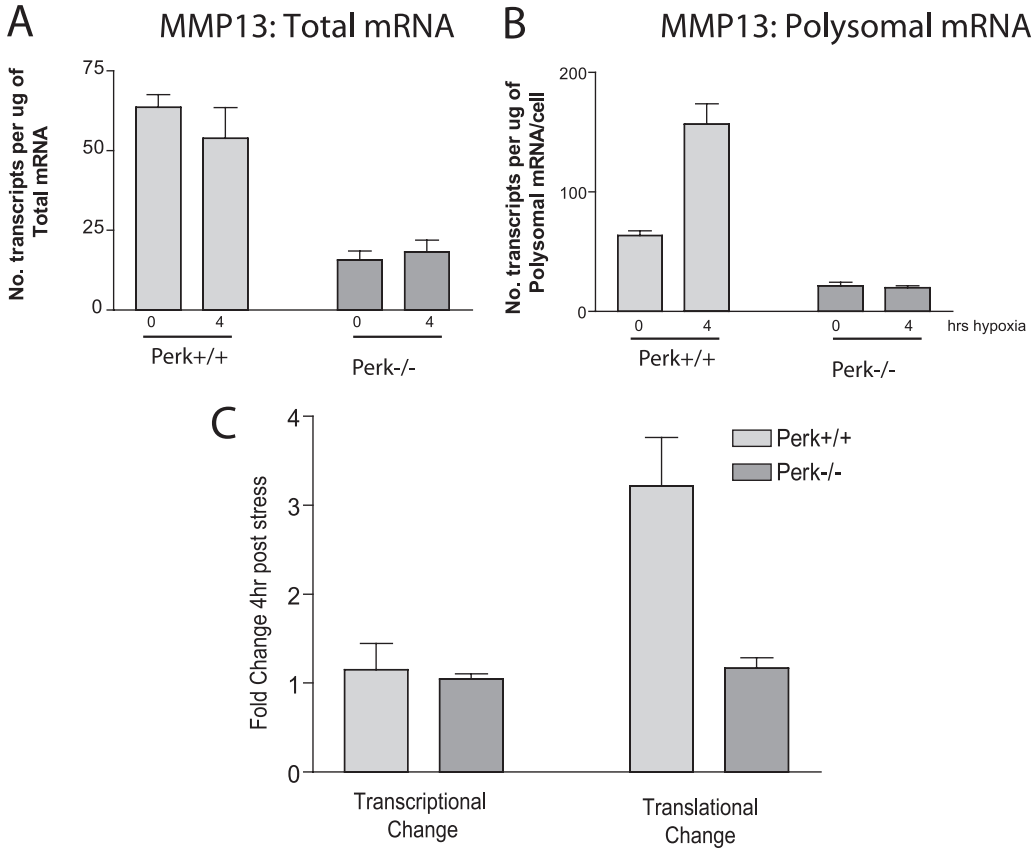

FIG. 5. MMP13 mRNA is more efficiently translated during hypoxia in Perk$^{+/+}$ cells. (A) Total mRNA expression is unaffected by hypoxia. Total RNA was isolated prior to sucrose gradient fractionation from hypoxia-treated (4 h) or normoxic (0 h) SV40-immortalized Perk$^{+/+}$ and Perk$^{-/-}$ cells, reverse transcribed, and quantified by real-time PCR. The quantities of each transcript are described as the number of transcripts isolated per microgram of total RNA. Each sample was independently normalized to a spiked internal control. Q-PCR analysis was replicated in triplicate. Results are representative of the averages ± SEM for three independent experiments. (B) MMP13 transcripts are enriched in the polysomes of Perk$^{+/+}$ cells during hypoxia. High-molecular-weight polysomes from hypoxia-treated (4 h) or normoxic (0 h) SV40-immortalized Perk$^{+/+}$ and Perk$^{-/-}$ cells were pooled (fractions 6 to 10), reverse transcribed, and quantified by real-time PCR. The quantities of each transcript are described as the number of transcripts isolated per microgram of polysomal RNA. Each sample was independently normalized to a spiked internal control. Q-PCR analysis was repeated in triplicate. Results are representative of the averages ± SEM for three independent experiments. (C) Perk$^{+/+}$ cells demonstrate induced translation of MMP13 during hypoxia. The transcriptional change (*n*-fold) was plotted as the number of MMP13 transcripts isolated per microgram of total RNA from hypoxia-treated (4 h) versus normoxic (0 h) cytoplasmic lysates. The translational change (*n*-fold) was plotted as the number of MMP13 transcripts isolated per microgram of polysomal RNA from hypoxia-treated (4 h) versus normoxic (0 h) lysates.

some fraction without a concomitant increase in the amount of mRNA in the total lysate (Fig. 5; see Fig. S1 in the supplemental material). Our initial microarray analysis demonstrated a modest increase in the steady-state levels of VCIP mRNA and a fourfold increase in polysome-associated mRNAs in Perk$^{+/+}$ cells upon hypoxic stress. Upon validation by Q-PCR, we noted a 10-fold difference in steady-state levels (Fig. 4A, compare 0 h and 4 h for Perk$^{+/+}$ and Perk$^{-/-}$; Fig. 4C) and a 20-fold translational induction in VCIP expression exclusively in Perk$^{+/+}$ cells (Fig. 4B, compare 0 h and 4 h for Perk$^{+/+}$ and Perk$^{-/-}$; Fig. 4C). It has been reported that VCIP exhibits a strong transcriptional induction in response to growth factors and cytokines in endothelial cells and epidermoid carcinomas (42); however, to our knowledge, this is the first report describing the posttranscriptional regulation of VCIP. Remarkably, Perk$^{-/-}$ cells were incapable of eliciting either a transcriptional or a translational induction in VCIP expression in response to hypoxic stress (Fig. 4). Similarly, Perk$^{+/+}$ cells demonstrated a differential translational induction of other genes involved in the regulation of angiogenesis, including MMP13, a metalloprotease that has been implicated in tumor invasion. The translational induction of MMP13 is evidenced by the recruitment of its mRNAs to the polysomes exclusively in Perk$^{+/+}$ cells in response to hypoxic stress (Fig. 5B, compare 0 h and 4 h for Perk$^{+/+}$ and Perk$^{-/-}$) without a concomitant increase in total cellular mRNAs (Fig. 5A, 0 h versus 4 h). Other validated candidates demonstrated similar translational induction in the absence of changes in total cellular mRNAs; these included Hyou1, Grb10, IGFBP2, and Col6a (see Fig. S1 in the supplemental material). Only 5.4% of the well-represented genes on the microarray demonstrated any translational dependence on Perk expression (genes induced >1.5-fold in the polysome fractions exclusively in Perk$^{+/+}$ cells without a concomitant >2-fold induction in the total mRNA relative to the number of total genes that demonstrated reliable signal by microarray, 1,254/25,055; Table 1). However, not all hypoxia-

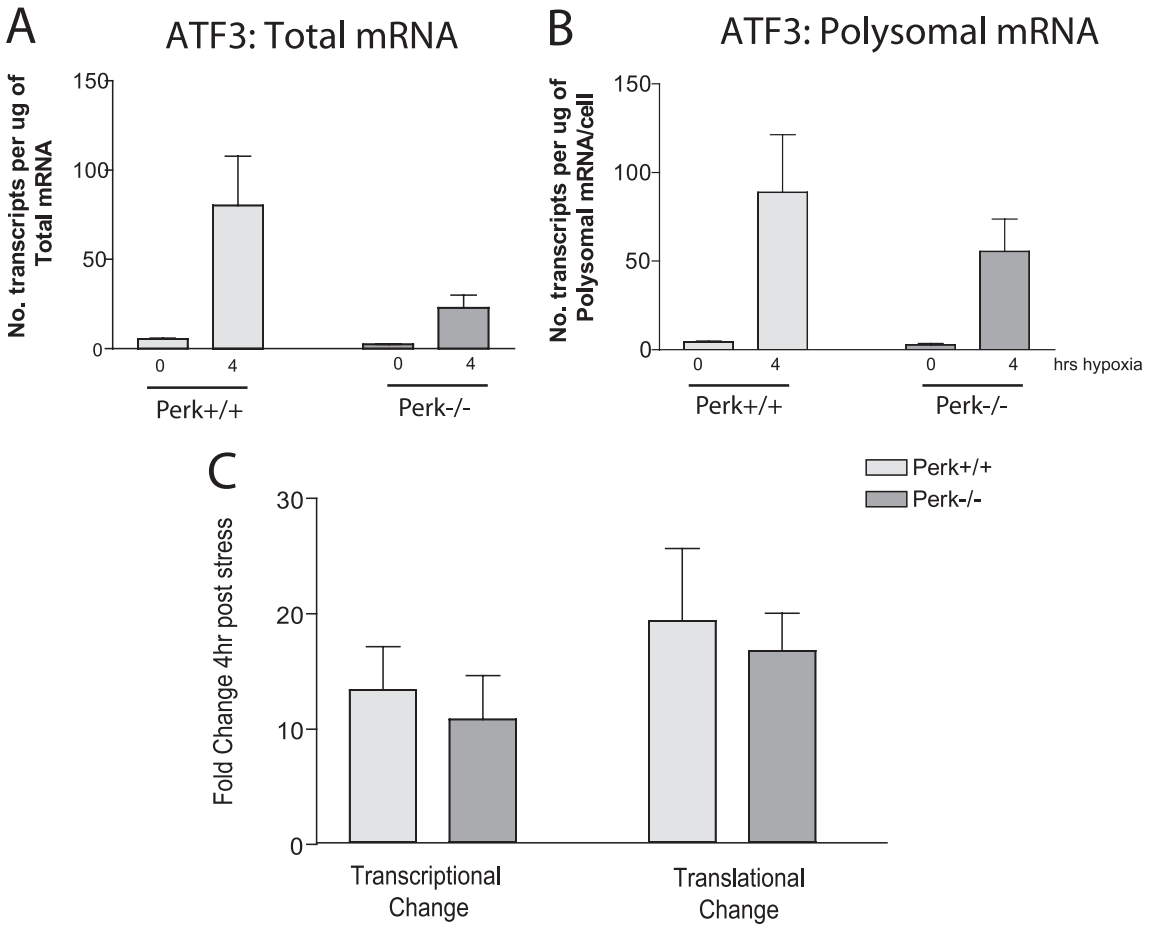

FIG. 6. Transcription and translation of ATF3 mRNA is not dependent on Perk activity during hypoxia. (A) ATF3 total mRNA expression is induced by hypoxic stress. Total RNA was isolated prior to sucrose gradient fractionation from hypoxia-treated (4 h) or normoxic (0 h) SV40-immortalized Perk$^{+/+}$ and Perk$^{-/-}$ cells, reverse transcribed, and quantified by real-time PCR. The quantities of each transcript are described as the number of transcripts isolated per microgram of total RNA. Each sample was independently normalized to a spiked internal control. Q-PCR analysis was replicated in triplicate. Results are representative of the averages ± SEM for three independent experiments. (B) ATF3 transcripts are enriched in the polysomes of Perk$^{+/+}$ and Perk$^{-/-}$ cells during hypoxia. High-molecular-weight polysomes from hypoxia-treated (4 h) or normoxic (0 h) SV40-immortalized Perk$^{+/+}$ and Perk$^{-/-}$ cells were pooled (fractions 6 to 10), reverse transcribed, and quantified by real-time PCR. The quantities of each transcript are described as the number of transcripts isolated per microgram of polysomal RNA. Each sample was independently normalized to a spiked internal control. Q-PCR analysis was repeated in triplicate. Results are representative of the averages ± SEM for three independent experiments. (C) Perk$^{+/+}$ and Perk$^{-/-}$ cells demonstrate induced transcription and translation of ATF3 during hypoxia. The transcriptional change (*n*-fold) was plotted as the number of ATF3 transcripts isolated per microgram of total RNA from hypoxia-treated (4 h) versus normoxic (0 h) cytoplasmic lysates. The translational change (*n*-fold) was plotted as the number of ATF3 transcripts isolated per microgram of polysomal RNA from hypoxia-treated (4 h) versus normoxic (0 h) lysates.

induced genes, such as ATF3, demonstrated a dependence on Perk expression (Fig. 6). Both Perk$^{+/+}$ and Perk$^{-/-}$ cells demonstrated a strong transcriptional (Fig. 4A and C) and translational (Fig. 6B and C) induction in ATF3 expression during hypoxic stress. We previously demonstrated that ATF3 responded to hypoxic stress by an increase in total cellular mRNA and by an increase in its polysome association (9); this study, however, demonstrates that induction of ATF3 in response to hypoxic stress is not dependent on Perk expression, a finding that has been corroborated by S. M. Nemetski and L. B. Gardner (submitted for publication).

As expected, large changes in steady-state mRNA levels in response to hypoxic stress were largely independent of Perk. We did observe, however, a reduced transcriptional (twofold) and translational (threefold) induction in the expression of CHOP/GADD153 in Perk$^{-/-}$ MEFs, which correlated with the reduced transcriptional induction of Myd116 (Gadd34) and CA6, two downstream targets of CHOP/GADD153 (Table 2). Previously, we demonstrated that hypoxic stress resulted in a substantial induction in CHOP expression (7), an observation that appears to be dependent on the activation of two UPR transcription factors, ATF4 (31) and ATF3 (46). The observation that CHOP expression was residually induced in Perk$^{-/-}$ MEFS suggests perhaps that ATF3 plays some role in the regulation of CHOP during hypoxic stress. Additionally, we noted a sevenfold and eightfold difference between Perk$^{+/+}$ and Perk$^{-/-}$ cells in the expression of metallothioneins 1 and 2 (MT1 and MT2), two members of a family of stress-induced proteins that play a critical role in protecting cells against metal toxicity and oxidants. The transcriptional induction of

TABLE 2. Total hypoxia-induced cellular changes in gene expression

Function	Transcriptional fold change		Gene name and description	Reference(s)
	$Perk^{+/+}$ cells	$Perk^{-/-}$ cells		
Angiogenesis	7.9	5.8	VEGF A	3, 29, 43
	4.9	3.1	Adrenomedullin 2	18, 45, 53
	4.7	4.4	Heme oxygenase 1	70
	3.6	2.2	Angiopoietin-like 6	
	3.6	3.3	Ephrin B2	47
	1.8	2.4	Angiomotin	
NO mediated	22.1	3.3	Metallothionein 1	8, 69
	18.7	2.4	Metallothionein 2	8, 69
UPR	13.8	15.4	hsp1A	
	10.1	26.6	hsp1A	
	4.5	6.3	hsp1	
	3.5	4.4	hsp70	
	6.3	2.2	Myd116 (Gadd34)	9
	1.9	2.5	DnaJ (Hsp40) homolog	
	11.5	6.0	Ddit3 (CHOP)	7, 9, 55
Regulation of transcription	15.6	18.6	ATF3	2, 9, 76
	3.0	2.0	ATF5	
	4.8	2.5	Max dimerization protein	
	3.4	1.8	Max protein	
Metabolism	8.6	2.6	CA6	
	6.3	1.9	Endothelial cell growth factor 1	
	3.2	5.2	Adenylate kinase 4	3, 95
	2.2	1.9	Aldehyde dehydrogenase 2	72
	2.0	2.0	6-Phosphofructo-2-kinase/fructose-2, 6-Biphosphatase 3	
	2.0	2.2	Phosphoglucomutase 2	
	3.4	4.0	Hexokinase 2	81, 64
	2.2	2.7	Pyruvate carboxylase	101
	3.0	1.8	Asparagine synthetase	
Response to DNA damage	10.9	5.6	DNA damage-inducible transcript 3	
	6.9	4.8	GADD45a	85
	5.1	8.3	DNA damage-inducible transcript 4	
Apoptosis	4.8	2.5	Max dimerization protein	
	3.4	18.6	NIP3	12, 30, 89
	2.5	2.8	BCL2-like 11 (apoptosis facilitator)	
mRNA processing and translation	2.2	2.5	Cytoplasmic polyadenylation element Binding protein 4	
	2.1	1.9	Dual-specificity phosphatase 3	

Results of Affymetrix MG430_2 microarray analysis used to identify steady-state changes in gene expression during hypoxia. Genespring 5.0 software was used to compare $Perk^{+/+}$ and $Perk^{-/-}$ 4 h total to 0 h total RNA to determine gene changes induced >2-fold. Genes were functionally clustered and referenced if previously identified in the literature. Only named genes are included in this list; expressed sequence tags were omitted.

MT1 in response to hypoxia has been previously described (69). More recently, Bi et al. described the activation of MT1 transcription upon the inhibition of protein synthesis with cycloheximide (8), suggesting a connection between the regulation of translation and the transcriptional induction of genes involved in the adaptive response to stress.

The 5′UTR of VCIP mediates internal initiation. Previous reports have established that VCIP gene expression is induced by growth factors and cytokines (42); however, the contribution of posttranscriptional regulation on VCIP expression had not yet been addressed. To ascertain if VCIP might be regulated in a manner similar to ATF4, through inhibitory upstream open reading frames (uORFs) in its 5′UTR, we searched the human VCIP 5′UTR and other mammalian orthologs for conserved uORFs and consistently found only one uORF present at the extreme 5′ region of its 5′UTR. Unlike ATF4, which has two conserved uORFs in its 5′UTR and is negatively regulated by the second uORF that causes readthrough of the canonical start codon (60, 92), we found no evidence for this mechanism of regulation in the VCIP 5′UTR. Interestingly, when we performed a sequence analysis of mammalian VCIP 5′UTRs, we noticed significant sequence homology between the human VCIP 5′UTR and those of other mammalian species (Fig. 7A). As hypoxic stress results in reduced cap-dependent translation initiation (4, 16, 50, 59, 91), internal ribosome recruitment to the VCIP 5′UTR may provide an alternative explanation for its translational induction during hypoxic stress. To test if VCIP contained an active

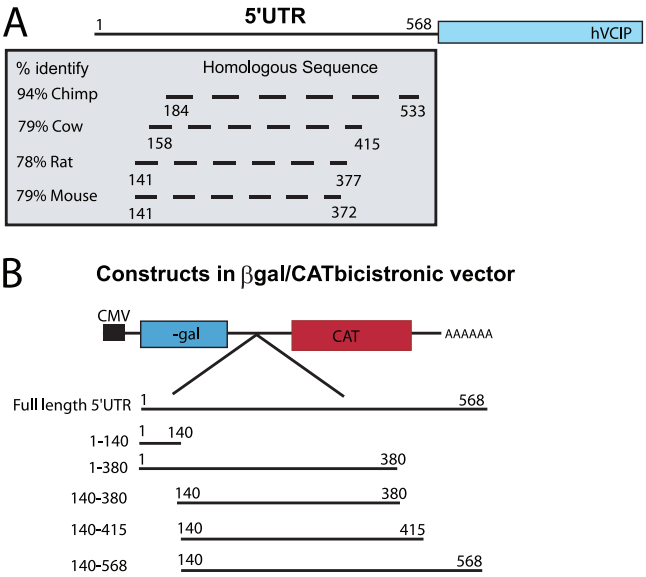

FIG. 7. VCIP 5′UTR is highly conserved. (A) The VCIP 5′UTR displays high conservation among several mammalian species. The various species are identified on the left with their percent identity to the human VCIP 5′UTR indicated. A dashed line specifies the areas within the 5′ UTR that share high homology with the human sequence. (B) A schematic of the various VCIP 5′UTR deletion constructs cloned into the β-Gal/CAT bicistronic vector.

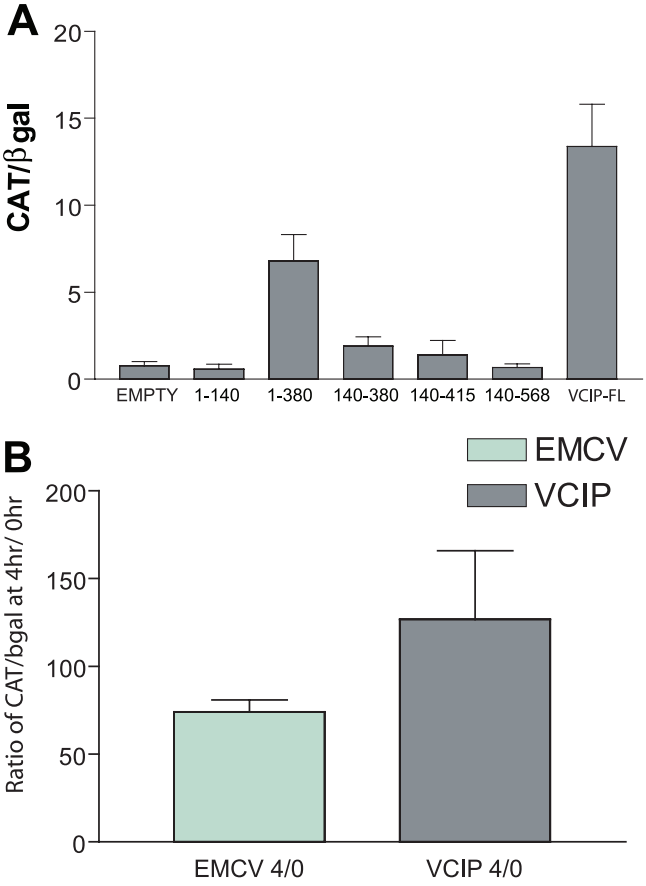

FIG. 8. VCIP 5′UTR contains a functional IRES. (A) U2OS cells were transfected with β-Gal/EMPTY/CAT control vector, the full-length VCIP 5′UTR, or various constructs containing portions of the VCIP 5′UTR cloned into the bicistronic β-Gal/CAT expression construct. The IRES activity is expressed as the CAT activity divided by the β-Gal activity measured using cell lysates taken 24 h posttransfection. The error bars represent the averages ± SEM from four to eight independent experiments. (B) U2OS cells were transfected with either the β-Gal/EMCV/CAT or β-Gal/VCIP/CAT bicistronic plasmid. Cells were either treated by hypoxia for 4 h at 24 h posttransfection or left untreated, and the relative IRES activity was determined for each IRES. The bars represent the averages ± SEM from three to five independent experiments.

IRES element, we cloned its 5′UTR into a β-Gal/CAT bicistronic vector (Fig. 7B). This construct is transcribed as a single capped mRNA with a short intercistronic sequence separating the 5′β-Gal cistron and the 3′CAT cistron. Translation of β-Gal is regulated by cap-dependent translation, whereas CAT translation can only be initiated by a bona fide IRES element capable of initiating cap-independent translation. The viral EMCV IRES cloned into the bicistronic vector was used as a positive control, whereas the empty bicistronic vector was included as a negative control. In addition, we created deletion mutants within the VCIP 5′UTR to help define the region(s) of IRES activity (Fig. 7B). Significant CAT activity was detected in extracts from cells transfected with the β-Gal/VCIP/CAT or β-Gal/EMCV/CAT bicistronic construct. As expected, no CAT expression was detected in cell extracts from β-Gal/EMPTY/CAT-transfected cells (Fig. 7A). Additionally, a small stem-loop structure was cloned upstream of the β-Gal cistron in the β-Gal/VCIP/CAT vector. This stem-loop structure creates an obstacle to the scanning ribosome, thereby inhibiting cap-dependent translation. Significant CAT expression was detected in lysates from cells transfected with the HP–β-Gal/VCIP/CAT expression vector (Fig. 8A) in the absence of any measurable β-Gal activity, suggesting that the VCIP 5′UTR mediates the production of CAT independent of β-Gal, as would be expected if an IRES element were present. Deletion constructs were created based on the homology pattern observed across species within the 5′UTR of VCIP (Fig. 7A). No homology was observed within the 1- to 140-bp region; similarly, CAT activity was ablated in this construct compared to the empty vector control, suggesting that, alone, this sequence does not contain an IRES sequence. Most of the homology identified within the 5′UTR spanned the sequence between bp 140 and 380, although CAT activity was only marginally active in this construct. Interestingly, only when the sequence spanning bp 1 to 140 was added to the sequence spanning bp 140 to 380 was significant IRES activity observed (Fig. 7A), suggesting a modular composition of the VCIP IRES. To ensure that VCIP IRES activity could not be explained by spurious splicing or cryptic promoter activity, we compared the quantities of β-Gal and CAT cistrons of the bicistronic mRNA by Q-PCR. The β-Gal/CAT bicistronic vector is transcribed as a single mRNA; thus, the ratio of β-Gal/CAT cistrons should equal 1. In the event that splicing or cryptic promoter activity is present within the 5′UTR of VCIP, CAT transcripts would be transcribed independently from β-Gal; thus, the quantity of CAT mRNA would exceed that of β-Gal mRNA, which could explain increased CAT activity in the absence of β-Gal expression. Q-PCR measurements demonstrated no differences in the proportion of β-Gal to CAT cistron RNA from cells trans-

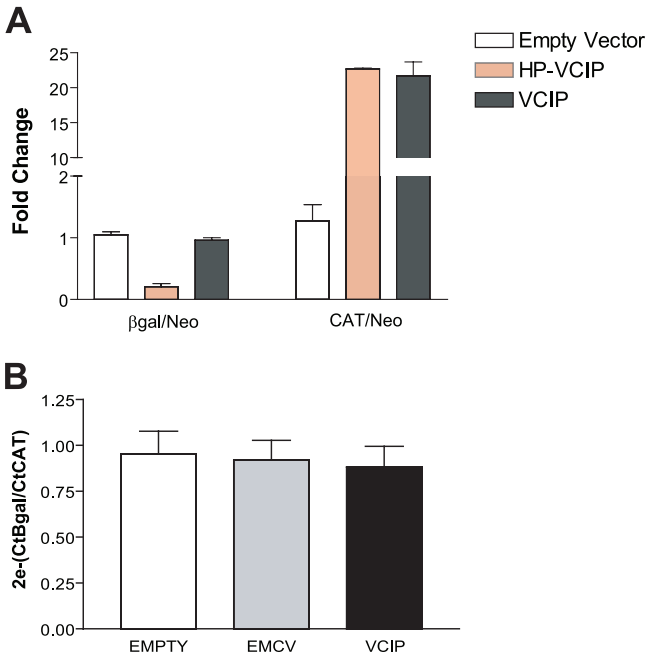

FIG. 9. VCIP 5′UTR does not contain cryptic promoter activity or evidence of spurious splicing. (A) U2OS cells were transfected with the β-Gal/EMPTY/CAT, β-Gal/VCIP/CAT, or HP–β-Gal/VCIP/CAT bicistronic plasmid. β-Gal and CAT activity was measured from cell lysates taken 24 h posttransfection and normalized to the number of transfected cells based on neomycin activity. Reported β-Gal and CAT activities are expressed relative to measurements obtained for β-Gal/EMPTY/CAT. Bars represent the averages ± SEM from three independent experiments. (B) Quantitative RT-PCR was performed with total RNA isolated from U2OS cells transfected with the β-Gal/EMCV/CAT, β-Gal/EMPTY/CAT, or β-Gal/VCIP/CAT bicistronic plasmid. Q-PCRs were carried out to quantify the number of β-Gal and CAT cistrons expressed in each plasmid. The CAT/β-Gal ratio was calculated as $2^{-[Ct(CAT) - Ct(\beta\text{-Gal})]}$, where Ct is the crossing point. The bars represent the means ± SEM from six to seven independent experiments performed in triplicate.

fected with either the EMCV, empty, or VCIP bicistronic vector (Fig. 8B), indicating that CAT activity measured in the VCIP bicistronic vector resulted from a bona fide cellular IRES within the 5′UTR.

IRES activity is maintained during hypoxia. To assess whether the putative VCIP IRES could function in a bicistronic context under hypoxic conditions, we transfected U2OS cells with β-Gal/EMCV/CAT or β-Gal/VCIP/CAT and placed these cells under normoxic or hypoxic conditions; the expression of β-Gal and CAT activity in cell extracts was measured. We observed that the CAT/β-Gal activity decreased approximately 25% in cells transfected with the β-Gal/EMCV/CAT vector (Fig. 9B). This effect is likely an overestimation of the true CAT/β-Gal activity due to the extreme stability of both β-Gal and CAT proteins. Most probably, EMCV IRES activity and global protein translation are similarly diminished in response to hypoxic stress. In contrast, the CAT/β-Gal activity measured in cells transfected with the β-Gal/VCIP/CAT construct remained high, suggesting that the VCIP IRES remains efficiently translated during hypoxic stress despite the substantial inhibition that occurs in protein translation. Moreover, U2OS cells cotransfected with the β-Gal/VCIP/CAT vector and a stress-inducible luciferase reporter fused to the 5′UTR of ATF4 demonstrate preferential association with polysomes during hypoxic stress (see Fig. S3 in the supplemental material), providing supporting evidence for the preferential translation of VCIP during hypoxic stress.

DISCUSSION

Tumor cell tolerance to hypoxia is an important determinant of the level of hypoxia which can be sustained within a given cell. This intrinsic property drives an adaptive response that results in increased cell survival during periods of heightened cellular stress and can elicit resistance to anticancer therapies. Recently, stress-tolerant cell lines were generated by means of repeated cycles of hypoxia and reoxygenation. Weinmann et al. established that hypoxia-resistant cell lines demonstrated cross-resistance to apoptosis induced by etoposide and UV irradiation (98). Additionally, stress-tolerant tumor cell lines generated by Yao et al. were more invasive and, when injected subcutaneously into nude mice, resulted in faster-growing tumors that demonstrated increased intratumoral angiogenesis (100).

The rapid and sustained inhibition of protein translation during hypoxic stress is thought to be one mechanism utilized by cells to promote hypoxia tolerance. The coordinated inhibition of protein translation, an energy-costly mechanism, is one energy-conserving strategy exploited by the cell when ATP levels are limited. Global translation inhibition is achieved upon activation of the ISR through the phosphorylation of eIF2α by the ER-resident kinase Perk (51). The luminal domain of Perk is negatively regulated by the ER chaperone BiP/Grp78, which maintains Perk in its inactive state in unstressed cells (6). During ER stress, the accumulation of unfolded proteins within the ER promotes the dissociation of BiP from the luminal domain of Perk to assist in protein folding. This dissociation results in the activation of Perk through oligomerization and *trans*-autophosphorylation of the cytoplasmic kinase domain (34). Similar to ER stress, hypoxia results in the activation of Perk and phosphorylation of eIF2α (51), leading to the attenuation of translation initiation and the paradoxical translational induction of ATF4 (9). ATF4 activates the induction of downstream UPR genes, including CHOP, BiP, and GADD34 (7, 9). The mechanism of Perk activation, however, has not yet been elucidated. Activation of the ISR constitutes one arm of a larger coordinated program called the UPR. Hypoxic stress similarly results in the activation of other branches of the UPR, including the activation of another ER transmembrane protein, IRE-1 (82). The role of hypoxic stress in the activation of the UPR has recently been thoroughly reviewed (52).

Perk has been implicated in promoting cell survival and adaptation in response to a variety of environmental stresses, including ER stress (31, 33) and hypoxia (7, 9, 51). In response to hypoxic stress, $Perk^{-/-}$ MEFs exhibit not only attenuated phosphorylation of eIF2α and reduced inhibition of protein synthesis but also reduced survival in vitro and in vivo. Tumors derived from cells with a compromised ISR ($Perk^{-/-}$ MEFs, HT29 cells expressing dn-PerkΔC, and cells expressing an unphosphorylatable knock-in mutant, $eIF2\alpha^{S51A}$) demonstrate reduced tumor cell viability compared to tumors with an intact ISR and result in smaller tumor growth (7).

A growing number of studies now support the idea that mechanisms that regulate global mRNA translation can simultaneously control the translation of individual genes necessary for cell survival and adaptation during stress (7, 9, 50). We previously demonstrated, through a collective analysis of data generated by microarray of polysome-associated mRNAs during prolonged hypoxic stress, the Perk-dependent translational regulation of ATF4, an important mediator of the ISR (9). Similar analyses have been previously employed to identify translationally regulated genes involved in the host cell response to poliovirus infection (48), T-cell activation (65), VHL expression (26), oncogenic signaling through Ras and Akt (79) and, in a recent time course experiment, hypoxic stress (50). The exact role that Perk plays in the progression of hypoxia tolerance, however, has not been fully elucidated. A previous microarray study identified several Perk-dependent transcriptionally induced changes in gene expression in an immortalized mouse hippocampal model for oxidative glutamatergic toxicity (61); however, a large-scale analysis of Perk-mediated changes in translation had not been completed prior to this study. Our analysis revealed the Perk-dependent preferential translation of a wide variety of proangiogenic genes, indicating that Perk may play a fundamental role in the translational regulation of a complex process that regulates the development of hypoxia tolerance through multiple pathways. It seems unlikely that any single gene product regulated by Perk is solely responsible for the control of tumor angiogenesis in response to hypoxic stress; rather, the orchestrated expression of many complementary gene products is likely responsible. In this study, we examined how one of our validated candidates, VCIP, an $\alpha_5\beta_1$ and $\alpha_v\beta_3$ integrin binding protein, is regulated at the translational level. The critical importance of VCIP gene function during angiogenesis is underscored by the observations that anti-VCIP antibodies block basic fibroblast growth factor (bFGF)- and VEGF-induced capillary morphogenesis (97) and that mouse embryos lacking the VCIP gene die between embryonic day 7 (E7) to E10.5 and demonstrate abnormal vascular development (20). The proangiogenic growth factors, bFGF and VEGF, are capable of eliciting a strong transcriptional induction in VCIP gene expression; however, the posttranscriptional regulation of VCIP had not been previously investigated. Our data establish that hypoxic stress in the absence of exogenous growth factors can initiate a 10-fold induction in the steady-state levels of VCIP transcripts. Moreover, VCIP mRNAs demonstrated a 20-fold translational induction as determined by their increased association with polysomes following hypoxic stress, suggesting VCIP expression is regulated by both transcriptional and posttranscriptional mechanisms. The VCIP 5′UTR is unusually long (568 bp) and surprisingly highly conserved across mammalian species. Unlike ATF4, the VCIP 5′UTR did not contain multiple conserved uORFs; therefore, the mechanism utilized to maintain its preferential translation during hypoxic stress is not likely ribosome shunting or reinitiation. Instead, our data support the presence of an active IRES element within its 5′UTR, which may in part explain its preferential translation when global translation is largely inhibited. Using deletion constructs of the hVCIP 5′UTR, we were able to determine that the VCIP IRES element is present between 1 and 380 bp. Removing the bp 1 to 140 from this construct, however, abolishes any IRES activity despite our observation that the sequence between bp 1 to 140 alone does not contain any IRES activity, suggesting that this sequence is necessary to determine the optimal secondary structure of the VCIP RNA for IRES-mediated translation. Numerous studies have identified hypoxia-responsive genes that employ IRES elements to maintain their translational priority during stress; these include the platelet-derived growth factor (PDGF) (5), HIF1α (54), VEGF (66, 90), BiP (62), TIE-2 (74), and ornithine decarboxylase (77) genes. The importance of IRES-mediated translation is revealed by the observation that mRNAs that contain IRES elements encode proteins that play important roles in cell growth, proliferation, differentiation, and the regulation of apoptosis, these being cellular programs that are often usurped by malignant cells (40). This observation suggests that IRES-mediated translation may be an important mechanism utilized by the cell to maintain and induce gene expression in order to mediate cellular adaptation and cell viability when cells are faced with stressful microenvironments. A possible connection between eIF2α phosphorylation and IRES translation has also been proposed. The activities of cat1, PDGF2, VEGF, and c-*myc* have been shown to increase either during differentiation or in response to various cellular stresses that increase the phosphorylation of eIF2α (21, 27). The mechanism for eIF2α phosphorylation-mediated IRES expression is not clear, as the phosphorylation of eIF2α results in the inhibition of ternary complex formation, a requirement for the initiation of all cellular mRNAs, including those that are regulated by cap-independent mechanisms. Whether eIF2α phosphorylation-sensitive IRES elements require specific *trans*-acting factors to mediate their translational activation during cellular stress has not been elucidated, but this requirement could help to explain their dependence on the phosphorylation of eIF2α. Alternatively, mRNAs with IRES elements may compete with other cellular mRNAs for the limited translational machinery to ensure their translational priority during times of reduced protein synthesis. Another explanation includes the possibility that eIF2α is not the only substrate of the Perk kinase and that, in fact, other molecules may be modulated by direct Perk phosphorylation. Interestingly, in response to ER stress, $eIF2\alpha^{S51A}$ cells failed to induce approximately one-third of the genes that are normally induced by ER stress (61), suggesting Perk is capable of mediating eIF2α-independent gene regulation. Recently, the bZIP transcription factor Nrf2 was identified as a second Perk substrate (17). In response to Perk activation, Nrf2 is phosphorylated by Perk, which promotes its dissociation from Keap1, thereby facilitating its translocation to the nucleus, where it binds and activates the transcription of antioxidant genes (93, 94). Aberrant Nrf2 regulation may help to explain why cells experience increased oxidative stress in the absence of Perk. Whether the translational regulation of the cohort of proangiogenic genes discussed here is done predominantly by eIF2α phosphorylation or whether they represent novel targets of Perk phosphorylation remains to be investigated.

The significance of Perk's role in regulating the translation of proangiogenic genes is emphasized by our observation that a wide variety of angiogenic genes involved in different braches of the angiogenic response demonstrated increased polysome association following hypoxic stress. Included in the Q-PCR-validated candidates is a matrix metalloproteinase, MMP13.

MMP-mediated extracellular matrix and basement membrane dissolution is an essential event for endothelial cell activation, migration, and capillary formation. More recent studies have implicated MMP expression in earlier steps of tumor evolution, including the stimulation of cell proliferation and modulation of angiogenesis (23, 24). The hMMP13 gene was originally identified in breast carcinoma, and its expression has since been related to other malignancies (25). The expression of hMMP13 has also been linked to the progression of rheumatoid arthritis in the synovial membrane, a disease that shares features with tumor invasion (58). Remarkably, hMMP13 transcripts are translationally silenced by the interaction of its 3′UTR and the nucleocytoplasmic shuttling protein TIAR (15); to our knowledge, however, we are the first to describe the translational induction of MMP13 during hypoxic stress. VCIP may be similarly regulated, as it has been demonstrated to contain an unusually long 3′UTR (>2 kb). We found it to contain two 15-lipoxygenase differentiation control element (15-LOX-DICE) sequences. The CU-rich 15-LOX-DICE is one of the best characterized 3′UTR control elements (80). Translational inhibition is mediated by the formation of a binary complex between the 15-LOX-DICE and KH domain proteins hnRNP E1 and K. Minimally, two 15-LOX-DICEs are required to confer translational repression of a transcript, and two to four repetitions per transcript is average. However, as many as 31 repetitions have been identified in a single 3′UTR (quail myelin protein mRNA) (80). In light of this observation, we are currently undertaking efforts to determine if the 3′UTR and 5′UTR of VCIP mutually regulate its posttranscriptional expression under aerobic and hypoxic conditions.

What is the physiological role for Perk in the translational regulation of these proteins in the development of hypoxia tolerance? Cells with a compromised ISR pathway demonstrate severe sensitivity to hypoxia (51) and pharmacological agents that promote ER stress (33). Our studies corroborated findings from Bi et al., as tumors derived from transformed Perk$^{-/-}$ MEFs are smaller than their wild-type counterparts. Furthermore, we made the observation that these tumors remained pale in color and did not appear to recruit angiogenic vessels as did wild-type tumors. In a mouse model of angiogenesis where tumor cells were cocultured with AP-expressing human microdermal endothelial cells, we made the observation that the tumor microenvironment imparted by Perk$^{-/-}$ cells resulted in abortive angiogenesis. Inappropriate levels of the constellation of ligands and receptors required during vessel maturation can result in the production of abnormal vessels. Maturation requires the recruitment of mural cells, the generation of an extracellular matrix, and specialization of the vessel wall for structural support (44). Expression of PDGF-B and ligation to its receptor (PDGFR-β) are required for the recruitment of pericyte progenitor cells and the eventual onset of vessel maturation (14, 44). The significance of PDGF-B during angiogenesis is underscored by the observation that PDGF-B-deficient mice die in utero at day E7.5 due to the inability to assemble mature vasculature in several organs (36, 44, 56, 57, 88). Furthermore, PDGF expression has been demonstrated to decrease over the progression of vessel maturation, indicating its requirement during the onset of maturation. Similar to hypoxic stress, cellular differentiation results in the inhibition of global protein synthesis, which correlates with the phosphorylation of eIF2α. Gerlitz et al. have demonstrated that IRES-mediated translation of PDGF during differentiation is dependent on the phosphorylation of eIF2α (27). Although we were unable to detect any changes in PDGF expression by microarray, our analysis did reveal a Perk-dependent 2.6-fold induction in the translational efficiency of its receptor, PDGFR-β, whereas its expression in Perk$^{-/-}$ MEFs was undetected relative to background (data not shown). Also critical for vessel formation and stabilization are the Tie receptors (Tie1 and Tie2). As mentioned previously, Tie2 is preferentially translated by an IRES element within its 5′UTR during hypoxic stress; however, whether IRES activity is dependent on eIF2α phosphorylation has not yet been determined.

Taken together, our data support the notion that Perk serves to fine-tune the translational efficiency of a subset of proangiogenic mRNAs during the course of hypoxic stress. Importantly, the inability to signal through Perk resulted in smaller tumor growth due in part to disregulated angiogenic signals that produced nonfunctional blood vessels. We propose that the translational regulation conferred by Perk in response to acute hypoxic stress represents a critical aspect in the development of hypoxia tolerance and in tumor growth. Results from this study further support the notion that Perk remains an attractive target for novel anticancer therapies.

ACKNOWLEDGMENTS

J.D.B. was supported by a CIHR-CGS doctoral award. This work was supported by a grant from the National Cancer Institute of Canada (to J.C.B.). Work done by D.R. and H.P.H. was supported by NIH grants ES08681 and DK47119. M.H. is a CIHR New Investigator. K.W. was supported by NIH grant HL079356.

REFERENCES

1. **Ala-aho, R., and V. M. Kahari.** 2005. Collagenases in cancer. Biochimie **87:**273–286.
2. **Ameri, K., E. M. Hammond, C. Culmsee, M. Raida, D. M. Katschinski, R. H. Wenger, E. Wagner, R. J. Davis, T. Hai, N. Denko, and A. L. Harris.** 17 July 2006. Induction of activating transcription factor 3 by anoxia is independent of p53 and the hypoxic HIF signalling pathway. Oncogene [Epub ahead of print.] doi:10.1038/sj.onc.1209781.
3. **Ameri, K., C. E. Lewis, M. Raida, H. Sowter, T. Hai, and A. L. Harris.** 2004. Anoxic induction of ATF-4 through HIF-1-independent pathways of protein stabilization in human cancer cells. Blood **103:**1876–1882.
4. **Arsham, A. M., J. J. Howell, and M. C. Simon.** 2003. A novel hypoxia-inducible factor-independent hypoxic response regulating mammalian target of rapamycin and its targets. J. Biol. Chem. **278:**29655–29660.
5. **Bernstein, J., O. Sella, S. Y. Le, and O. Elroy-Stein.** 1997. PDGF2/c-sis mRNA leader contains a differentiation-linked internal ribosomal entry site (D-IRES). J. Biol. Chem. **272:**9356–9362.
6. **Bertolotti, A., Y. Zhang, L. M. Hendershot, H. P. Harding, and D. Ron.** 2000. Dynamic interaction of BiP and ER stress transducers in the unfolded-protein response. Nat. Cell Biol. **2:**326–332.
7. **Bi, M., C. Naczki, M. Koritzinsky, D. Fels, J. Blais, N. Hu, H. Harding, I. Novoa, M. Varia, J. Raleigh, D. Scheuner, R. J. Kaufman, J. Bell, D. Ron, B. G. Wouters, and C. Koumenis.** 2005. ER stress-regulated translation increases tolerance to extreme hypoxia and promotes tumor growth. EMBO J. **24:**3470–3481.
8. **Bi, Y., G. X. Lin, L. Millecchia, and Q. Ma.** 2006. Superinduction of metallothionein I by inhibition of protein synthesis: role of a labile repressor in MTF-1 mediated gene transcription. J. Biochem. Mol. Toxicol. **20:**57–68.
9. **Blais, J. D., V. Filipenko, M. Bi, H. P. Harding, D. Ron, C. Koumenis, B. G. Wouters, and J. C. Bell.** 2004. Activating transcription factor 4 is translationally regulated by hypoxic stress. Mol. Cell. Biol. **24:**7469–7482.
10. **Bornstein, P., T. R. Kyriakides, Z. Yang, L. C. Armstrong, and D. E. Birk.** 2000. Thrombospondin 2 modulates collagen fibrillogenesis and angiogenesis. J. Investig. Dermatol. Symp. Proc. **5:**61–66.
11. **Brown, J. M., and A. J. Giaccia.** 1998. The unique physiology of solid tumors: opportunities (and problems) for cancer therapy. Cancer Res. **58:**1408–1416.
12. **Bruick, R. K.** 2000. Expression of the gene encoding the proapoptotic Nip3 protein is induced by hypoxia. Proc. Natl. Acad. Sci. USA **97:**9082–9087.

13. **Cattaruzza, S., M. Schiappacassi, A. Ljungberg-Rose, P. Spessotto, D. Perissinotto, M. Morgelin, M. T. Mucignat, A. Colombatti, and R. Perris.** 2002. Distribution of PG-M/versican variants in human tissues and de novo expression of isoform V3 upon endothelial cell activation, migration, and neoangiogenesis in vitro. J. Biol. Chem. **277:**47626–47635.
14. **Cho, H., T. Kozasa, C. Bondjers, C. Betsholtz, and J. H. Kehrl.** 2003. Pericyte-specific expression of Rgs5: implications for PDGF and EDG receptor signaling during vascular maturation. FASEB J. **17:**440–442.
15. **Chua, P. K., M. E. Melish, Q. Yu, R. Yanagihara, K. S. Yamamoto, and V. R. Nerurkar.** 2003. Elevated levels of matrix metalloproteinase 9 and tissue inhibitor of metalloproteinase 1 during the acute phase of Kawasaki disease. Clin. Diagn. Lab. Immunol. **10:**308–314.
16. **Connolly, E., S. Braunstein, S. Formenti, and R. J. Schneider.** 2006. Hypoxia inhibits protein synthesis through a 4E-BP1 and elongation factor 2 kinase pathway controlled by mTOR and uncoupled in breast cancer cells. Mol. Cell. Biol. **26:**3955–3965.
17. **Cullinan, S. B., D. Zhang, M. Hannink, E. Arvisais, R. J. Kaufman, and J. A. Diehl.** 2003. Nrf2 is a direct PERK substrate and effector of PERK-dependent cell survival. Mol. Cell. Biol. **23:**7198–7209.
18. **Damert, A., M. Machein, G. Breier, M. Q. Fujita, D. Hanahan, W. Risau, and K. H. Plate.** 1997. Up-regulation of vascular endothelial growth factor expression in a rat glioma is conferred by two distinct hypoxia-driven mechanisms. Cancer Res. **57:**3860–3864.
19. **de Fraipont, F., A. C. Nicholson, J. J. Feige, and E. G. Van Meir.** 2001. Thrombospondins and tumor angiogenesis. Trends Mol. Med. **7:**401–407.
20. **Escalante-Alcalde, D., L. Hernandez, H. Le Stunff, R. Maeda, H.-S. Lee, Jr-Gang-Cheng, V. A. Sciorra, I. Daar, S. Spiegel, A. J. Morris, and C. L. Stewart.** 2003. The lipid phosphatase LPP3 regulates extra-embryonic vasculogenesis and axis patterning. Development **130:**4623–4637.
21. **Fernandez, P. M., S. O. Tabbara, L. K. Jacobs, F. C. Manning, T. N. Tsangaris, A. M. Schwartz, K. A. Kennedy, and S. R. Patierno.** 2000. Overexpression of the glucose-regulated stress gene GRP78 in malignant but not benign human breast lesions. Breast Cancer Res. Treat. **59:**15–26.
22. **Firth, J. D., B. L. Ebert, C. W. Pugh, and P. J. Ratcliffe.** 1994. Oxygen-regulated control elements in the phosphoglycerate kinase 1 and lactate dehydrogenase A genes: similarities with the erythropoietin 3′ enhancer. Proc. Natl. Acad. Sci. USA **91:**6496–6500.
23. **Folgueras, A. R., A. M. Pendas, L. M. Sanchez, and C. Lopez-Otin.** 2004. Matrix metalloproteinases in cancer: from new functions to improved inhibition strategies. Int. J. Dev. Biol. **48:**411–424.
24. **Freije, J. M., M. Balbin, A. M. Pendas, L. M. Sanchez, X. S. Puente, and C. Lopez-Otin.** 2003. Matrix metalloproteinases and tumor progression. Adv. Exp. Med. Biol. **532:**91–107.
25. **Freije, J. M., I. Diez-Itza, M. Balbin, L. M. Sanchez, R. Blasco, J. Tolivia, and C. Lopez-Otin.** 1994. Molecular cloning and expression of collagenase-3, a novel human matrix metalloproteinase produced by breast carcinomas. J. Biol. Chem. **269:**16766–16773.
26. **Galban, S., J. Fan, J. L. Martindale, C. Cheadle, B. Hoffman, M. P. Woods, G. Temeles, J. Brieger, J. Decker, and M. Gorospe.** 2003. von Hippel-Lindau protein-mediated repression of tumor necrosis factor alpha translation revealed through use of cDNA arrays. Mol. Cell. Biol. **23:**2316–2328.
27. **Gerlitz, G., R. Jagus, and O. Elroy-Stein.** 2002. Phosphorylation of initiation factor-2 alpha is required for activation of internal translation initiation during cell differentiation. Eur. J. Biochem. **269:**2810–2819.
28. **Graeber, T. G., C. Osmanian, T. Jacks, D. E. Housman, C. J. Koch, S. W. Lowe, and A. J. Giaccia.** 1996. Hypoxia-mediated selection of cells with diminished apoptotic potential in solid tumours. Nature **379:**88–91.
29. **Greijer, A. E., P. van der Groep, D. Kemming, A. Shvarts, G. L. Semenza, G. A. Meijer, M. A. van de Wiel, J. A. Belien, P. J. van Diest, and E. van der Wall.** 2005. Up-regulation of gene expression by hypoxia is mediated predominantly by hypoxia-inducible factor 1 (HIF-1). J. Pathol. **206:**291–304.
30. **Griffin, J. L., C. Rae, R. M. Dixon, G. K. Radda, and P. M. Matthews.** 1998. Excitatory amino acid synthesis in hypoxic brain slices: does alanine act as a substrate for glutamate production in hypoxia? J. Neurochem. **71:**2477–2486.
31. **Harding, H. P., I. Novoa, Y. Zhang, H. Zeng, R. Wek, M. Schapira, and D. Ron.** 2000. Regulated translation initiation controls stress-induced gene expression in mammalian cells. Mol. Cell **6:**1099–1108.
32. **Harding, H. P., H. Zeng, Y. Zhang, R. Jungries, P. Chung, H. Plesken, D. D. Sabatini, and D. Ron.** 2001. Diabetes mellitus and exocrine pancreatic dysfunction in *Perk*$^{-/-}$ mice reveals a role for translational control in secretory cell survival. Mol. Cell **7:**1153–1163.
33. **Harding, H. P., Y. Zhang, A. Bertolotti, H. Zeng, and D. Ron.** 2000. Perk is essential for translational regulation and cell survival during the unfolded protein response. Mol. Cell **5:**897–904.
34. **Harding, H. P., Y. Zhang, and D. Ron.** 1999. Protein translation and folding are coupled by an endoplasmic-reticulum-resident kinase. Nature **397:**271–274.
35. **Harding, H. P., Y. Zhang, H. Zeng, I. Novoa, P. D. Lu, M. Calfon, N. Sadri, C. Yun, B. Popko, R. Paules, D. F. Stojdl, J. C. Bell, T. Hettmann, J. M. Leiden, and D. Ron.** 2003. An integrated stress response regulates amino acid metabolism and resistance to oxidative stress. Mol. Cell **11:**619–633.
36. **Hellstrom, M., M. Kalen, P. Lindahl, A. Abramsson, and C. Betsholtz.** 1999. Role of PDGF-B and PDGFR-beta in recruitment of vascular smooth muscle cells and pericytes during embryonic blood vessel formation in the mouse. Development **126:**3047–3055.
37. **Hochachka, P. W., L. T. Buck, C. J. Doll, and S. C. Land.** 1996. Unifying theory of hypoxia tolerance: molecular/metabolic defense and rescue mechanisms for surviving oxygen lack. Proc. Natl. Acad. Sci. USA **93:**9493–9498.
38. **Hockel, M., K. Sclenger, H. Hamm, P. G. Knapstein, R. Hohenfellner, and H. P. Rosler.** 1996. Five-year experience with combined operative and radiotherapeutic treatment of recurrent gynecologic tumors infiltrating the pelvic wall. Cancer **77:**1918–1933.

38a. **Holcik, M., T. Graber, S. M. Lewis, C. A. Lefebvre, E. Lacasse, and S. Baird.** 2005. Spurious splicing within the XIAP 5′ UTR occurs in the Rluc/Fluc but not the betagal/CAT bicistronic reporter system. RNA **11:**1605–1609.

39. **Holcik, M., C. Lefebvre, C. Yeh, T. Chow, and R. G. Korneluk.** 1999. A new internal-ribosome-entry-site motif potentiates XIAP-mediated cytoprotection. Nat. Cell Biol. **1:**190–192.
40. **Holcik, M., N. Sonenberg, and R. G. Korneluk.** 2000. Internal ribosome initiation of translation and the control of cell death. Trends Genet. **16:**469–473.
41. **Humtsoe, J. O., R. A. Bowling, Jr., S. Feng, and K. K. Wary.** 2005. Murine lipid phosphate phosphohydrolase-3 acts as a cell-associated integrin ligand. Biochem. Biophys. Res. Commun. **335:**906–919.
42. **Humtsoe, J. O., S. Feng, G. D. Thakker, J. Yang, J. Hong, and K. K. Wary.** 2003. Regulation of cell-cell interactions by phosphatidic acid phosphatase 2b/VCIP. EMBO J. **22:**1539–1554.
43. **Iyer, N. V., L. E. Kotch, F. Agani, S. W. Leung, E. Laughner, R. H. Wenger, M. Gassmann, J. D. Gearhart, A. M. Lawler, A. Y. Yu, and G. L. Semenza.** 1998. Cellular and developmental control of O2 homeostasis by hypoxia-inducible factor 1 alpha. Genes Dev. **12:**149–162.
44. **Jain, R. K.** 2003. Molecular regulation of vessel maturation. Nat Med. **9:**685–693.
45. **Jiang, B. H., J. Z. Zheng, S. W. Leung, R. Roe, and G. L. Semenza.** 1997. Transactivation and inhibitory domains of hypoxia-inducible factor 1alpha. Modulation of transcriptional activity by oxygen tension. J. Biol. Chem. **272:**19253–19260.
46. **Jiang, H. Y., S. A. Wek, B. C. McGrath, D. Lu, T. Hai, H. P. Harding, X. Wang, D. Ron, D. R. Cavener, and R. C. Wek.** 2004. Activating transcription factor 3 is integral to the eukaryotic initiation factor 2 kinase stress response. Mol. Cell. Biol. **24:**1365–1377.
47. **Jogi, A., J. Vallon-Christersson, L. Holmquist, H. Axelson, A. Borg, and S. Pahlman.** 2004. Human neuroblastoma cells exposed to hypoxia: induction of genes associated with growth, survival, and aggressive behavior. Exp. Cell Res. **295:**469–487.
48. **Johannes, G., M. S. Carter, M. B. Eisen, P. O. Brown, and P. Sarnow.** 1999. Identification of eukaryotic mRNAs that are translated at reduced cap binding complex eIF4F concentrations using a cDNA microarray. Proc. Natl. Acad. Sci. USA **96:**13118–13123.
49. **Klenotic, P. A., F. L. Munier, L. Y. Marmorstein, and B. Anand-Apte.** 2004. Tissue inhibitor of metalloproteinases-3 (TIMP-3) is a binding partner of epithelial growth factor-containing fibulin-like extracellular matrix protein 1 (EFEMP1). Implications for macular degenerations. J. Biol. Chem. **279:**30469–30473.
50. **Koritzinsky, M., M. G. Magagnin, T. van den Beucken, R. Seigneuric, K. Savelkouls, J. Dostie, S. Pyronnet, R. J. Kaufman, S. A. Weppler, J. W. Voncken, P. Lambin, C. Koumenis, N. Sonenberg, and B. G. Wouters.** 2006. Gene expression during acute and prolonged hypoxia is regulated by distinct mechanisms of translational control. EMBO J. **25:**1114–1125.
51. **Koumenis, C., C. Naczki, M. Koritzinsky, S. Rastani, A. Diehl, N. Sonenberg, A. Koromilas, and B. G. Wouters.** 2002. Regulation of protein synthesis by hypoxia via activation of the endoplasmic reticulum kinase PERK and phosphorylation of the translation initiation factor eIF2α. Mol. Cell. Biol. **22:**7405–7416.
52. **Koumenis, C., and B. G. Wouters.** 2006. "Translating" tumor hypoxia: unfolded protein response (UPR)-dependent and UPR-independent pathways. Mol. Cancer Res. **4:**423–436.
53. **Ladoux, A., and C. Frelin.** 2000. Coordinated up-regulation by hypoxia of adrenomedullin and one of its putative receptors (RDC-1) in cells of the rat blood-brain barrier. J. Biol. Chem. **275:**39914–39919.
54. **Lang, K. J., A. Kappel, and G. J. Goodall.** 2002. Hypoxia-inducible factor-1alpha mRNA contains an internal ribosome entry site that allows efficient translation during normoxia and hypoxia. Mol. Biol. Cell **13:**1792–1801.
55. **Lee, P. J., B. H. Jiang, B. Y. Chin, N. V. Iyer, J. Alam, G. L. Semenza, and A. M. Choi.** 1997. Hypoxia-inducible factor-1 mediates transcriptional activation of the heme oxygenase-1 gene in response to hypoxia. J. Biol. Chem. **272:**5375–5381.
56. **Leveen, P., M. Pekny, S. Gebre-Medhin, B. Swolin, E. Larsson, and C. Betsholtz.** 1994. Mice deficient for PDGF B show renal, cardiovascular, and hematological abnormalities. Genes Dev. **8:**1875–1887.
57. **Lindahl, P., B. R. Johansson, P. Leveen, and C. Betsholtz.** 1997. Pericyte loss and microaneurysm formation in PDGF-B-deficient mice. Science **277:**242–245.

58. **Lindy, O., Y. T. Konttinen, T. Sorsa, Y. Ding, S. Santavirta, A. Ceponis, and C. Lopez-Otin.** 1997. Matrix metalloproteinase 13 (collagenase 3) in human rheumatoid synovium. Arthritis Rheum. **40:**1391–1399.
59. **Liu, L., T. P. Cash, R. G. Jones, B. Keith, C. B. Thompson, and M. C. Simon.** 2006. Hypoxia-induced energy stress regulates mRNA translation and cell growth. Mol. Cell **21:**521–531.
60. **Lu, P. D., H. P. Harding, and D. Ron.** 2004. Translation reinitiation at alternative open reading frames regulates gene expression in an integrated stress response. J. Cell Biol. **167:**27–33.
61. **Lu, P. D., C. Jousse, S. J. Marciniak, Y. Zhang, I. Novoa, D. Scheuner, R. J. Kaufman, D. Ron, and H. P. Harding.** 2004. Cytoprotection by pre-emptive conditional phosphorylation of translation initiation factor 2. EMBO J. **23:**169–179.
62. **Macejak, D. G., and P. Sarnow.** 1991. Internal initiation of translation mediated by the 5′ leader of a cellular mRNA. Nature **353:**90–94.
63. **MacGregor, G. R., G. P. Nolan, S. Fiering, M. Roederer, and L. A. Herzenberg.** 1991. Use of E. coli lacZ (b-galactosidase) as a reporter gene. Humana Press, Inc., Clifton, N.J.
64. **Mathupala, S. P., A. Rempel, and P. L. Pedersen.** 2001. Glucose catabolism in cancer cells: identification and characterization of a marked activation response of the type II hexokinase gene to hypoxic conditions. J. Biol. Chem. **276:**43407–43412.
65. **Mikulits, W., B. Pradet-Balade, B. Habermann, H. Beug, J. A. Garcia-Sanz, and E. W. Mullner.** 2000. Isolation of translationally controlled mRNAs by differential screening. FASEB J. **14:**1641–1652.
66. **Miller, D. L., J. A. Dibbens, A. Damert, W. Risau, M. A. Vadas, and G. J. Goodall.** 1998. The vascular endothelial growth factor mRNA contains an internal ribosome entry site. FEBS Lett. **434:**417–420.
67. **Mooney, D. J., K. Sano, P. M. Kaufmann, K. Majahod, B. Schloo, J. P. Vacanti, and R. Langer.** 1997. Long-term engraftment of hepatocytes transplanted on biodegradable polymer sponges. J. Biomed. Mater. Res. **37:**413–420.
68. **Murdaca, J., C. Treins, M. N. Monthouel-Kartmann, R. Pontier-Bres, S. Kumar, E. Van Obberghen, and S. Giorgetti-Peraldi.** 2004. Grb10 prevents Nedd4-mediated vascular endothelial growth factor receptor-2 degradation. J. Biol. Chem. **279:**26754–26761.
69. **Murphy, B. J., G. K. Andrews, D. Bittel, D. J. Discher, J. McCue, C. J. Green, M. Yanovsky, A. Giaccia, R. M. Sutherland, K. R. Laderoute, and K. A. Webster.** 1999. Activation of metallothionein gene expression by hypoxia involves metal response elements and metal transcription factor-1. Cancer Res. **59:**1315–1322.
70. **Nguyen, S. V., and W. C. Claycomb.** 1999. Hypoxia regulates the expression of the adrenomedullin and HIF-1 genes in cultured HL-1 cardiomyocytes. Biochem. Biophys. Res. Commun. **265:**382–386.
71. **Nor, J. E., M. C. Peters, J. B. Christensen, M. M. Sutorik, S. Linn, M. K. Khan, C. L. Addison, D. J. Mooney, and P. J. Polverini.** 2001. Engineering and characterization of functional human microvessels in immunodeficient mice. Lab. Investig. **81:**453–463.
72. **O'Rourke, J. F., C. W. Pugh, S. M. Bartlett, and P. J. Ratcliffe.** 1996. Identification of hypoxically inducible mRNAs in HeLa cells using differential-display PCR. Role of hypoxia-inducible factor-1. Eur. J. Biochem. **241:**403–410.
73. **Ozawa, K., Y. Tsukamoto, O. Hori, Y. Kitao, H. Yanagi, D. M. Stern, and S. Ogawa.** 2001. Regulation of tumor angiogenesis by oxygen-regulated protein 150, an inducible endoplasmic reticulum chaperone. Cancer Res. **61:**4206–4213.
74. **Park, E. H., J. M. Lee, J. D. Blais, J. C. Bell, and J. Pelletier.** 2005. Internal translation initiation mediated by the angiogenic factor Tie2. J. Biol. Chem. **280:**20945–20953.
75. **Pettersen, E. O., N. O. Juul, and O. W. Ronning.** 1986. Regulation of protein metabolism of human cells during and after acute hypoxia. Cancer Res. **46:**4346–4351.
76. **Price, B. D., and S. K. Calderwood.** 1992. Gadd45 and Gadd153 messenger RNA levels are increased during hypoxia and after exposure of cells to agents which elevate the levels of the glucose-regulated proteins. Cancer Res. **52:**3814–3817.
77. **Pyronnet, S., L. Pradayrol, and N. Sonenberg.** 2000. A cell cycle-dependent internal ribosome entry site. Mol. Cell **5:**607–616.
78. **Qi, J. H., Q. Ebrahem, and B. Anand-Apte.** 2003. Tissue inhibitor of metalloproteinases-3 and Sorsby fundus dystrophy. Adv. Exp. Med. Biol. **533:**97–105.
79. **Rajasekhar, V. K., A. Viale, N. D. Socci, M. Wiedmann, X. Hu, and E. C. Holland.** 2003. Oncogenic Ras and Akt signaling contribute to glioblastoma formation by differential recruitment of existing mRNAs to polysomes. Mol. Cell **12:**889–901.
80. **Reimann, I., A. Huth, H. Thiele, and B. J. Thiele.** 2002. Suppression of 15-lipoxygenase synthesis by hnRNP E1 is dependent on repetitive nature of LOX mRNA 3′-UTR control element DICE. J. Mol. Biol. **315:**965–974.
81. **Reisdorph, R., and R. Lindahl.** 2001. Aldehyde dehydrogenase 3 gene regulation: studies on constitutive and hypoxia-modulated expression. Chem. Biol. Interact. **130–132:**227–233.
82. **Romero-Ramirez, L., H. Cao, D. Nelson, E. Hammond, A. H. Lee, H. Yoshida, K. Mori, L. H. Glimcher, N. C. Denko, A. J. Giaccia, Q. T. Le, and A. C. Koong.** 2004. XBP1 is essential for survival under hypoxic conditions and is required for tumor growth. Cancer Res. **64:**5943–5947.
83. **Russo, V. C., B. S. Schutt, E. Andaloro, S. I. Ymer, A. Hoeflich, M. B. Ranke, L. A. Bach, and G. A. Werther.** 2005. Insulin-like growth factor binding protein-2 binding to extracellular matrix plays a critical role in neuroblastoma cell proliferation, migration, and invasion. Endocrinology **146:**4445–4455.
84. **Scheuner, D., B. Song, E. McEwen, C. Liu, R. Laybutt, P. Gillespie, T. Saunders, S. Bonner-Weir, and R. J. Kaufman.** 2001. Translational control is required for the unfolded protein response and in vivo glucose homeostasis. Mol. Cell **7:**1165–1176.
85. **Schmidt-Kastner, R., C. Aguirre-Chen, T. Kietzmann, I. Saul, R. Busto, and M. D. Ginsberg.** 2004. Nuclear localization of the hypoxia-regulated pro-apoptotic protein BNIP3 after global brain ischemia in the rat hippocampus. Brain Res. **1001:**133–142.
86. **Sherman-Baust, C. A., A. T. Weeraratna, L. B. Rangel, E. S. Pizer, K. R. Cho, D. R. Schwartz, T. Shock, and P. J. Morin.** 2003. Remodeling of the extracellular matrix through overexpression of collagen VI contributes to cisplatin resistance in ovarian cancer cells. Cancer Cell **3:**377–386.
87. **Shweiki, D., A. Itin, D. Soffer, and E. Keshet.** 1992. Vascular endothelial growth factor induced by hypoxia may mediate hypoxia-initiated angiogenesis. Nature **359:**843–845.
88. **Soriano, P.** 1994. Abnormal kidney development and hematological disorders in PDGF beta-receptor mutant mice. Genes Dev. **8:**1888–1896.
89. **Sowter, H. M., P. J. Ratcliffe, P. Watson, A. H. Greenberg, and A. L. Harris.** 2001. HIF-1-dependent regulation of hypoxic induction of the cell death factors BNIP3 and NIX in human tumors. Cancer Res. **61:**6669–6673.
90. **Stein, I., A. Itin, P. Einat, R. Skaliter, Z. Grossman, and E. Keshet.** 1998. Translation of vascular endothelial growth factor mRNA by internal ribosome entry: implications for translation under hypoxia. Mol. Cell. Biol. **18:**3112–3119.
91. **Tinton, S. A., and P. M. Buc-Calderon.** 1999. Hypoxia increases the association of 4E-binding protein 1 with the initiation factor 4E in isolated rat hepatocytes. FEBS Lett. **446:**55–59.
92. **Vattem, K. M., and R. C. Wek.** 2004. Reinitiation involving upstream ORFs regulates ATF4 mRNA translation in mammalian cells. Proc. Natl. Acad. Sci. USA **101:**11269–11274.
93. **Venugopal, R., and A. K. Jaiswal.** 1996. Nrf1 and Nrf2 positively and c-Fos and Fra1 negatively regulate the human antioxidant response element-mediated expression of NAD(P)H:quinone oxidoreductase1 gene. Proc. Natl. Acad. Sci. USA **93:**14960–14965.
94. **Venugopal, R., and A. K. Jaiswal.** 1998. Nrf2 and Nrf1 in association with Jun proteins regulate antioxidant response element-mediated expression and coordinated induction of genes encoding detoxifying enzymes. Oncogene **17:**3145–3156.
95. **Vihanto, M. M., J. Plock, D. Erni, B. M. Frey, F. J. Frey, and U. Huynh-Do.** 2005. Hypoxia up-regulates expression of Eph receptors and ephrins in mouse skin. FASEB J. **19:**1689–1691.
96. **Warnakulasuriyarachchi, D., S. Cerquozzi, H. H. Cheung, and M. Holcik.** 2004. Translational induction of the inhibitor of apoptosis protein HIAP2 during endoplasmic reticulum stress attenuates cell death and is mediated via an inducible internal ribosome entry site element. J. Biol. Chem. **279:**17148–17157.
97. **Wary, K. K., and J. O. Humtsoe.** 2005. Anti-lipid phosphate phosphohydrolase-3 (LPP3) antibody inhibits bFGF- and VEGF-induced capillary morphogenesis of endothelial cells. Cell Commun. Signal. **3:**9.
98. **Weinmann, M., V. Jendrossek, D. Guner, B. Goecke, and C. Belka.** 2004. Cyclic exposure to hypoxia and reoxygenation selects for tumor cells with defects in mitochondrial apoptotic pathways. FASEB J. **18:**1906–1908.
99. **Wimmer-Kleikamp, S. H., and M. Lackmann.** 2005. Eph-modulated cell morphology, adhesion and motility in carcinogenesis. IUBMB Life **57:**421–431.
100. **Yao, K., J. A. Gietema, S. Shida, M. Selvakumaran, X. Fonrose, N. B. Haas, J. Testa, and P. J. O'Dwyer.** 2005. In vitro hypoxia-conditioned colon cancer cell lines derived from HCT116 and HT29 exhibit altered apoptosis susceptibility and a more angiogenic profile in vivo. Br. J. Cancer **93:**1356–1363.
101. **Yasuda, S., S. Arii, A. Mori, N. Isobe, W. Yang, H. Oe, A. Fujimoto, Y. Yonenaga, H. Sakashita, and M. Imamura.** 2004. Hexokinase II and VEGF expression in liver tumors: correlation with hypoxia-inducible factor 1 alpha and its significance. J. Hepatol. **40:**117–123.
102. **Zhang, P., B. McGrath, S. Li, A. Frank, F. Zambito, J. Reinert, M. Gannon, K. Ma, K. McNaughton, and D. R. Cavener.** 2002. The PERK eukaryotic initiation factor 2α kinase is required for the development of the skeletal system, postnatal growth, and the function and viability of the pancreas. Mol. Cell. Biol. **22:**3864–3874.